

# Headwater channel dynamics in semiarid rangelands, Colorado high plains, USA

**Gregory E. Tucker**<sup>†</sup>

*Cooperative Institute for Research in Environmental Sciences (CIRES) and Department of Geological Sciences, University of Colorado, Boulder, Colorado 80309, USA*

**Lee Arnold**<sup>‡</sup>

*School of Geography and the Environment, University of Oxford, South Parks Road, Oxford OX1 3QY, UK*

**Rafael L. Bras**<sup>§</sup>

**Homero Flores**<sup>#</sup>

*Department of Civil and Environmental Engineering, Massachusetts Institute of Technology, Cambridge, Massachusetts 02139, USA*

**Erkan Istanbuluoglu**<sup>††</sup>

*Department of Geosciences, University of Nebraska, Lincoln, Nebraska 68588, USA*

**Peter Solyom**<sup>\*\*</sup>

*School of Geography and the Environment, University of Oxford, South Parks Road, Oxford OX1 3QY, UK*

## ABSTRACT

Incised ephemeral channels provide a window into the fluvial processes that help sculpt rangeland landscapes. This paper presents observations of ephemeral channels and valley networks in the high plains of Colorado, USA, with an eye toward painting a picture of the ingredients that must be included in mathematical models of landscape evolution in such environments. Channel incision in the study area is driven by summer thunderstorms, which can with reasonable frequency (3–5 yr) generate boundary shear stresses high enough to penetrate the highly resistant vegetation armor, but only within erosional hot spots where hydraulic forces are amplified by channel constriction and locally steep gradients. Focusing of erosion at these hot spots (which correspond to knickpoints and channel heads) is amplified by the small areal footprint and short “erosional reach” of most convective storms. Upstream migration of knickpoints creates a pattern of short, active channel reaches separated by unchanneled or weakly channeled, fully vegetated stable

reaches. Based on our observations, we interpret the necessary and sufficient conditions leading to the observed channel forms and dynamics as: (1) a resistant vegetation layer overlying an erodible substrate, which sets up a conditional instability through which erosional perturbations can grow by positive feedback; (2) high flow variability; (3) moderate to high substrate cohesion; and (4) a high volume fraction of fine-grained erodible material. Concave-upward valley long profiles are interpreted as a trade-off between downstream-increasing flood frequency and downstream-decreasing flood effectiveness. The observed process dynamics imply that long-term rates of valley incision should be especially sensitive to climatic oscillations between episodes of drought and warm-season convective rainfall.

**Keywords:** arroyos, climate, erosion, gullies, networks, streams.

## INTRODUCTION

Understanding erosion and sediment transport in rangeland landscapes is important for a variety of reasons. From the perspective of land management, effective erosion control requires an understanding of the nature, frequency, and magnitude of the climatic, hydrologic, biotic, and geomorphic drivers. From the perspective of long-term

landscape evolution, a quantitative understanding of the “rules of the landscape” is needed in order to answer questions such as: What are the frequency and magnitude properties of sediment movement, and how do these change with spatial scale? How sensitive are rates of sediment movement and topographic change to climatic, tectonic, or human forcing? What interpretations of the Quaternary landscape-change record are consistent with the mechanics and chemistry of the driving processes? In addition, in the particular case of the high plains bordering the Colorado Front Range, which we investigate here, quantitative models of rangeland dynamics are needed to test the plausibility of the hypothesis that climatic oscillation has driven late Cenozoic accelerated denudation along the margins of the Colorado Rockies (e.g., Gregory and Chase, 1994; Zhang et al., 2001).

In this contribution, we focus on the dynamics of low-order ephemeral channel networks. Ephemeral headwater channel systems are important to understand because they are primary conduits for water and sediment movement in arid and semiarid landscapes. They also tend to be highly dynamic, with gully systems capable of growing rapidly into formerly unchanneled valleys (e.g., Montgomery and Dietrich, 1992; Prosser et al., 1994; Bull, 1997; Fanning, 1999; Tucker and Slingerland, 1997; Boardman et al., 2003; Istanbuluoglu et al., 2004) and generating high sediment yields.

<sup>†</sup>E-mail: gtucker@cires.colorado.edu.

<sup>‡</sup>E-mail: lee.arnold@st-peters.ox.ac.uk.

<sup>§</sup>E-mail: rlbras@mit.edu.

<sup>#</sup>E-mail: homefc@mit.edu.

<sup>††</sup>E-mail: erkan@unl.edu.

<sup>\*\*</sup>E-mail: peter.solyom@geog.ox.ac.uk.

Modern gully networks are often attributed to human impacts (typically livestock grazing; e.g., Graf, 1988; Fanning, 1999). For example, Dietrich et al. (1993) argued that the extent of channels in a California grassland catchment could only be explained by past vegetation disturbance; the extent of the mapped channel network corresponded to an overland flow erosion threshold of 16–32 Pa, while a flume study in the same catchment suggested an effective erosion threshold of over 100 Pa under complete grass cover (Prosser et al., 1995). Montgomery and Dietrich (1992) interpreted the extension of gullies in the same setting as a response to overgrazing. Yet the fact that this and other gully networks typically occupy preexisting valley networks (as opposed to hillslopes) suggests that periodic sediment evacuation by channel extension is a common natural process that does not require human disturbance (e.g., Reneau et al., 1990). In order to understand the dynamics of valley network extension and retreat over geologic time scales, and the sensitivity of the system to environmental change (e.g., Rinaldo et al., 1995; Tucker and Slingerland, 1997), we need to understand the natural trigger factors for channel growth and retreat. To what degree is channel network extension driven by rare, intense storms, as opposed to episodes of vegetation disturbance due to drought, grazing, and disease? What controls the frequency and magnitude of extension events? And what are the implications of these controls for catchment sensitivity to climate change?

Here, we report observations from ephemeral channel networks in Colorado, USA, to address these questions and provide data for testing quantitative models. Our aim is to paint a picture of the morphology, driving processes, and dynamics of low-order ephemeral streams in this region. Analyses of aerial photographs and recent erosion events provide insights into the tempo of channel extension. Paleohydrologic reconstructions provide evidence for the magnitude of shear stresses generated during convective summer storms, and the relative frequency of these events. From these observations, inferences are drawn regarding the geomorphic impact of localized, high-intensity storm cells. Collectively, these observations and inferences provide a necessary backdrop for developing process-based mathematical models to describe channel network dynamics in this type of setting.

## BACKGROUND

The term rangeland is usually defined on the basis of vegetation (predominantly grasses, shrubs, and similar groups) or land use (suitable

for grazing animals but not arable agriculture) or both. Here, we use a looser, geomorphically based definition: terrain with low to moderate relief in which either present-day or glacial maximum climate supported a climax vegetation of predominantly low-growing species such as shrubs and grasses. This definition includes the high plains and plateau landscapes of the North American west, much of southern Africa, the central Asian steppes, large areas of the Australian lowlands, Mediterranean regions, South American pampas, and similar regions.

The geomorphology of rangelands is commonly characterized by ephemeral or intermittent stream channels and unchanneled valleys. Dry channels, variously called “gullies,” “arroyos,” “wadis,” or other regional terms, are common. Whatever the name, ephemeral channels in rangelands are often incised into valley-floor alluvium or occasionally bedrock (e.g., Cooke and Reeves, 1976; Graf, 1983; Bull, 1997; Prosser and Slade, 1994; Boardman et al., 2003). Some of these incised dry-land channels are continuous, while others (generally in smaller basins) are discontinuous, with entrenched reaches separated by nonincised valley segments (Bull, 1997). Here we use the term arroyo to refer generally to incised, ephemeral channels with steep sidewalls and a rectilinear to U-shaped cross section. (Note that by including incised ephemeral channels of all sizes, we depart from the definition of Graf [1988], who preferred the term “gully” for smaller channels. However, “gully” is commonly used to refer to any small, incised channel regardless of morphology, and is therefore too general for our purposes.)

Arroyo networks are zones of concentrated geomorphic activity, and an understanding of sediment budgets and landscape sensitivity therefore requires a quantitative understanding of their governing mechanisms. A great deal has been written on arroyo networks, particularly those in the western United States. The bulk of the literature, however, has concentrated on understanding the trigger factors (e.g., grazing, subtle climate change, or other causes) for widespread arroyo incision in the American west near the close of the nineteenth century (e.g., Antevs, 1952; Cooke and Reeves, 1976; Graf, 1983). Although “ultimate causes” have proven difficult to untangle, it is clear that there usually is a strong correlation between the advent of intensive grazing and widespread channel incision (e.g., Graf, 1988), but equally, in some parts of the world, ancient filled channels indicate that incision has occurred repeatedly during the late Quaternary, indicating that intensive livestock grazing is not the only possible trigger (e.g., Waters and Haynes, 2001).

A number of studies have focused on documenting patterns of channel change in dry lands, using repeat channel surveys, space-time substitution, and other methods. These studies resulted in a valuable database of observations and led to the development of conceptual models to describe a typical “arroyo cycle.” Schumm (1977) argued that arroyos commonly undergo a phase of rapid incision, followed by widening and subsequent aggradation as stream power decreases and sediment supply from side walls increases. This view was modified by Elliott et al. (1999) to include the possibility of subsequent phases of incision. Leopold (1951) correlated arroyo trenching in the southwestern United States with a period of increased rainfall intensity and decreased mean rainfall, and argued that this subtle climate change was sufficient to drive widespread incision. This view was challenged by Schumm and Parker (1973) and Paton and Schumm (1975), who argued on the basis of field observations and laboratory experiments that repeated episodes of incision and infilling can occur due to internal dynamics within a drainage network and do not necessarily require direct external forcing. Likewise, Schumm et al. (1987) found experimental evidence for a “complex response” to external forcing, in which a single base-level fall stimulated a series of complex, localized erosion-deposition reverberations that were superimposed on an overall exponential-like decline in sediment yield. Slingerland and Snow (1988) later established a theoretical basis for these fluctuations. In a similar vein, Bull (1997) developed a conceptual model for discontinuous ephemeral streams in which deposition of a fan-like deposit below a discontinuous channel leads to a gradual increase in gradient, until stream power is sufficient to drive renewed incision.

Collectively, the evidence for complex internal dynamics in a drainage network implies that past episodes of incision or infilling will not necessarily provide much information about environmental change. It does not, however, imply that channel incision is unpredictable, but simply that the proximal causes are at least partly internal (e.g., variations in channel width, gradient, stream power, etc.) rather than external.

Despite these advances, we still lack a quantitative, process-based theory for arroyo formation and development, though recent models have begun to address this issue (Howard, 1999; Kirkby and Bull, 2000; Istanbuloglu et al., 2004, 2005) and related problems, such as the role of vegetation dynamics in ephemeral channel networks (Collins et al., 2004). To develop and test a comprehensive, process-based theory, we require quantitative observations of arroyo hydrology, kinematics (rates of

morphologic change), vegetation patterns, and erosion and sedimentation rates. Here we report on observations collected from arroyo networks in central and southern Colorado, USA. These observations, together with inferences drawn from numerical modeling, point toward (1) an episodic pattern of arroyo initiation and growth in both time and space, (2) the importance of intense, convective storms in driving channel incision and advance, and (3) the central role of rangeland vegetation as an erosion mediator.

## FIELD SETTING

We focus on two field areas in the Colorado high plains. The first lies in the Red Creek and Dry Creek drainage basins, just east of the central Colorado Front Range and south of the city of Colorado Springs (Figs. 1A and 1B). Topography comprises a mixture of rugged foothills, reflecting the progressive dissection of deformed Paleozoic through late Mesozoic sedimentary rocks, and open rangelands. The landscape is adorned with remnants of Quaternary gravel-capped terrace surfaces, which generally decrease in age, altitude, and extent from west to east. Valley networks in the more cohesive soils and/or lithologies are typically veined with

steep-walled incised channels. The bulk of the underlying lithologies are sedimentary rocks related to the Cretaceous Western Interior Seaway. Mean annual rainfall in nearby Colorado Springs is 41 cm, with a late summer maximum. Most summer rain arrives in the form of convective thunderstorms, which can generate short-term (1–5 min) peak rainfall intensities ranging from a few tens of millimeters per hour to as high as 300 mm/h within the core of the cell (e.g., Goodrich et al., 1997; Bull et al., 1999; Ogden et al., 2000).

The second site lies along the northern margin of the Purgatoire River, a large tributary of the Arkansas, and includes Big Arroyo (40 km<sup>2</sup>; tributary of Timpas Creek) and Taylor Arroyo (125 km<sup>2</sup>; tributary of the Purgatoire River) drainage basins (Figs. 1A and 1C). The landscape is one of open, gently rolling rangelands interrupted by prominent bedrock scarps. Vegetation is primarily a mix of grassland and open piñon-juniper woodland. The Purgatoire River and the lower parts of its tributaries occupy steep-walled bedrock canyons. The bedrock geology consists of a subhorizontal sequence of Jurassic through late Cretaceous sedimentary rocks. To the northeast, an anticline belonging to the Apishapa Arch forms a dome slivered by

steep-walled box canyons. Mean annual rainfall is ~30 cm, with a July maximum. Each year the area receives ~60 convective thunderstorms on average (von Guerard et al., 1987). Figure 2 shows the cumulative (one day) rainfall pattern of a typical summer thunderstorm system. All or most channels, except the Purgatoire itself, are ephemeral and often clearly incised into the underlying alluvium or bedrock. Based on U.S. Geological Survey flow records, Big and Taylor Arroyos convey an average of 5–6 flash floods each year. An overview of the hydrology and physiography of the area is given by von Guerard et al. (1987).

## CHANNEL MORPHOLOGY

### Occurrence and Lithology

A variety of different channel forms has been observed in these field areas and similar environments in the Colorado piedmont. As discussed above, we focus here on ephemeral valley networks containing incised channels with distinct, steep to vertical side walls (Fig. 3). Often, these incised channels are discontinuous, with segments terminating at their upstream end in an abrupt head scarp abutting

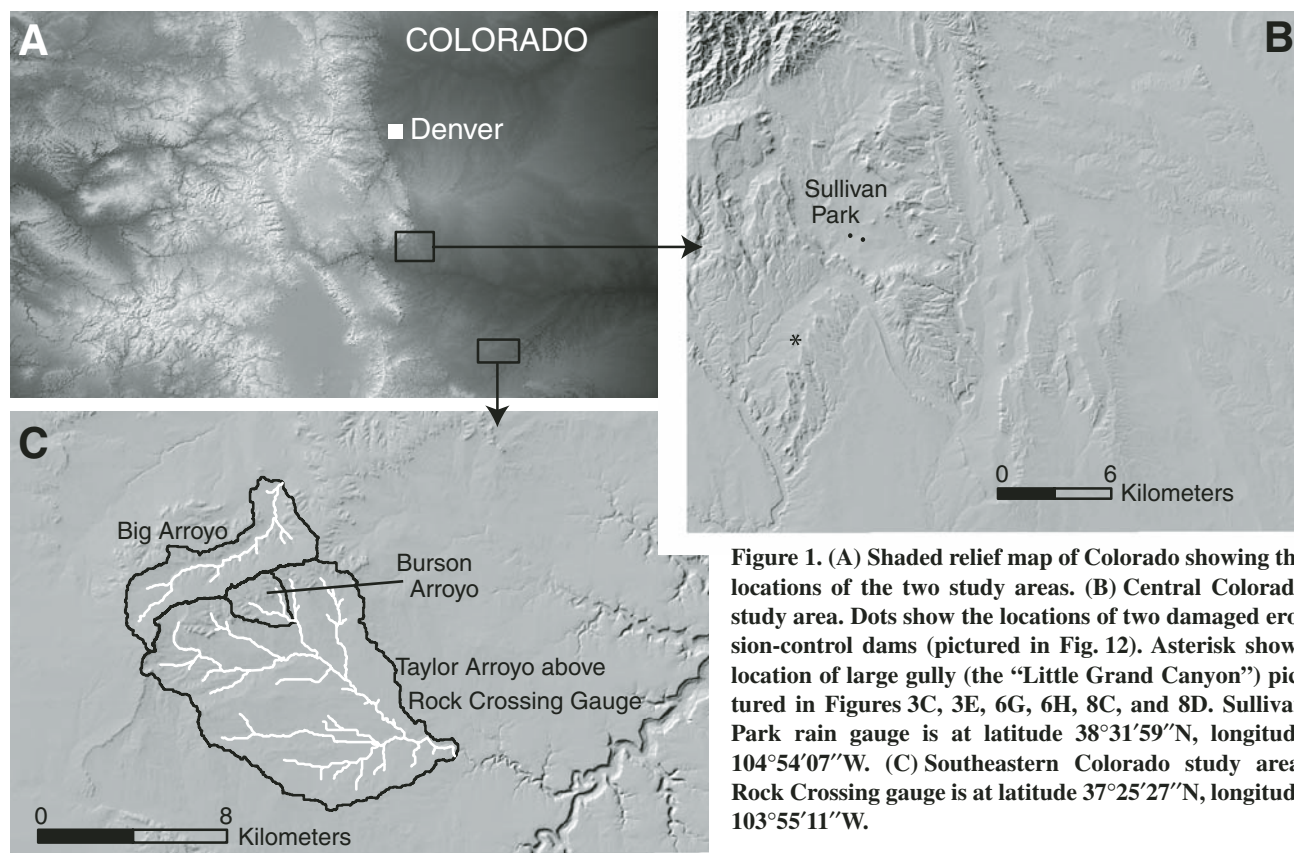


**Figure 1.** (A) Shaded relief map of Colorado showing the locations of the two study areas. (B) Central Colorado study area. Dots show the locations of two damaged erosion-control dams (pictured in Fig. 12). Asterisk shows location of large gully (the “Little Grand Canyon”) pictured in Figures 3C, 3E, 6G, 6H, 8C, and 8D. Sullivan Park rain gauge is at latitude 38°31′59″N, longitude 104°54′07″W. (C) Southeastern Colorado study area. Rock Crossing gauge is at latitude 37°25′27″N, longitude 103°55′11″W.

a plunge pool (cf. Bull, 1997). Based on aerial photograph analysis and field reconnaissance, it is clear that these channels occur predominantly in cohesive valley alluvium and/or shale bedrock. Texture analysis shows that valley fills typically range from clay to sandy loam; the average median grain size from 41 field samples is 0.03 mm (medium silt;  $\phi = 5.9 \pm 1.8$ ; Flores, 2004). Incised channels are rare or absent in more competent lithologies (e.g., the Fort Hayes limestone member of the Niobrara Formation), though they often occur in alluvial valley fills that overly these lithologies. Where channels have been observed to cut into bedrock, the bedrock is typically shale-rich. In several cases, we have observed vertical walls of alluvium overhanging fissile shale bedrock, suggesting that the fill is often more cohesive than the shale (Fig. 3C). Steep-walled ephemeral channels are also rare on the Quaternary gravel-capped pediments that drape the skirts of the Front Range, presumably due to lack of cohesion in the gravels (Istanbulluoglu et al., 2005).

### Cross-Sectional Geometry and Side-Wall Stability

By definition, the channels investigated here are rectilinear to U-shaped in cross section. Side walls often show a near-vertical wall section above a sloping rampart (Fig. 3C). Vertical wall height is correlated to substrate cohesion (Fig. 4), and Istanbulluoglu et al. (2005) showed that this material control on wall stability can have a first-order impact on the morphological style of channel propagation. Unlike the valley and channel floors, and to a lesser extent ramparts, steep channel walls are nearly always devoid of vegetation (Fig. 3). Vegetation on channel floors ranges from essentially absent (Figs. 3C and 3E) to a full cover of woody and herbaceous riparian species (Fig. 3B).

### Channel Heads

We have observed three types of channel head morphology, which often intergrade with one another:

1. Channels or channel segments that terminate abruptly with steep, vertical headcuts (ranging from “large step” to “large headcut” in the classification of Dietrich and Dunne, 1993, and corresponding to the “abrupt” channel-head morphology of Oostwoud Wijdenes et al., 1999) (Figs. 3A and 3D).

2. Channels in which a narrower, shallower reach extends tens of meters above a prominent, broader and deeper head scarp. In these cases, the head scarp is typically supported by tree

roots or by a resistant rock stratum. This morphology corresponds to the “rilled-abrupt” classification of Oostwoud Wijdenes et al. (1999).

3. Flights of arcuate, discontinuous steps (Fig. 5). Steps often lack discernible banks; where present, these rarely extend more than a few meters below the step. Step flights often occur up-valley from a longer channel segment showing morphology type 1 or 2. In other cases, they grade gradually downstream into increasingly long discontinuous channel segments. Evidence from historical air photos (discussed in the following) shows that step flights are sometimes precursors to continuous incised channel segments.

### Longitudinal Profiles

The longitudinal valley profiles are generally straight to moderately concave-upward (typical concavity index between 0.1 and 0.4, as defined by Whipple and Tucker, 1999), and often show lithologic control (Fig. 6). In some cases, the upward-concave profiles extend upstream of the modern channel network. For example, in the valley shown in Figures 6C and 6D, the upper portion of the valley is decorated with a flight of steps (Fig. 5), but is otherwise unchanneled.

Discontinuous incised channels with lengths on the order of a few hundred meters are often deepest at their head, and grade into the valley surface at their terminus (Figs. 3C and 6G). In some cases, the lower portion of the incised channel grades into a fan within the valley. Next, we explore the origins of this pattern.

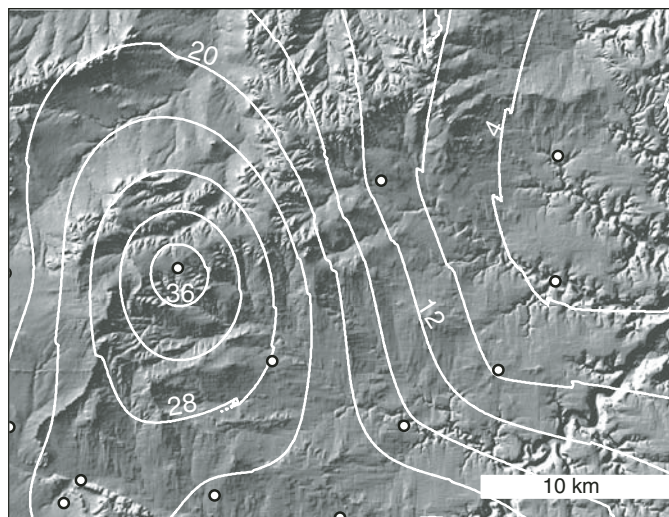


**Figure 2.** Map showing 24 h precipitation total over Big and Burson Arroyos on 8 August 2003. Contour interval is in mm. White circles show positions of tipping-bucket rain gauges. The  $e$ -folding distance for decay of rainfall total from the storm center is ~10–15 km. Peak precipitation was recorded at Burson Well, latitude 37°30'04"N, longitude 104°03'20"W.

### RATES AND PATTERNS OF CHANNEL GROWTH

#### Cut-and-Fill Cycles

Several lines of evidence indicate that arroyos in the study area undergo alternating periods of channel incision and valley/channel aggradation, a behavior that is common to arroyo systems elsewhere in the western United States (e.g., Patton and Schumm, 1975; Cooke and Reeves, 1976; Graf, 1983; Bull, 1997; Elliott et al., 1999; Waters and Haynes, 2001). Unchanneled valley segments often alternate with incised channels (Fig. 7). Ancient, infilled channels are commonly observed in channel side walls (Fig. 3C). Optically stimulated luminescence (OSL) dating of basal fills in paleochannels in the study area yields ages ranging from early to late Holocene (Arnold, 2006).

#### Historic Aerial Photograph Analysis

In order to estimate rates of gully-head advance, we compared historic and modern aerial photographs covering two quarter-quadrangles (3.75' × 3.75') that fall within the northern study area. The northeast quadrant of the U.S. Geological Survey (USGS) Pierce Gulch 7.5' quadrangle and the northwest quadrant of the Steele Hollow 7.5' quadrangle were chosen because they include arroyo networks that we have examined closely in the field. Two photograph series were used: 1937 USDA (U.S. Department of Agriculture) 1:20,000 photographs, and

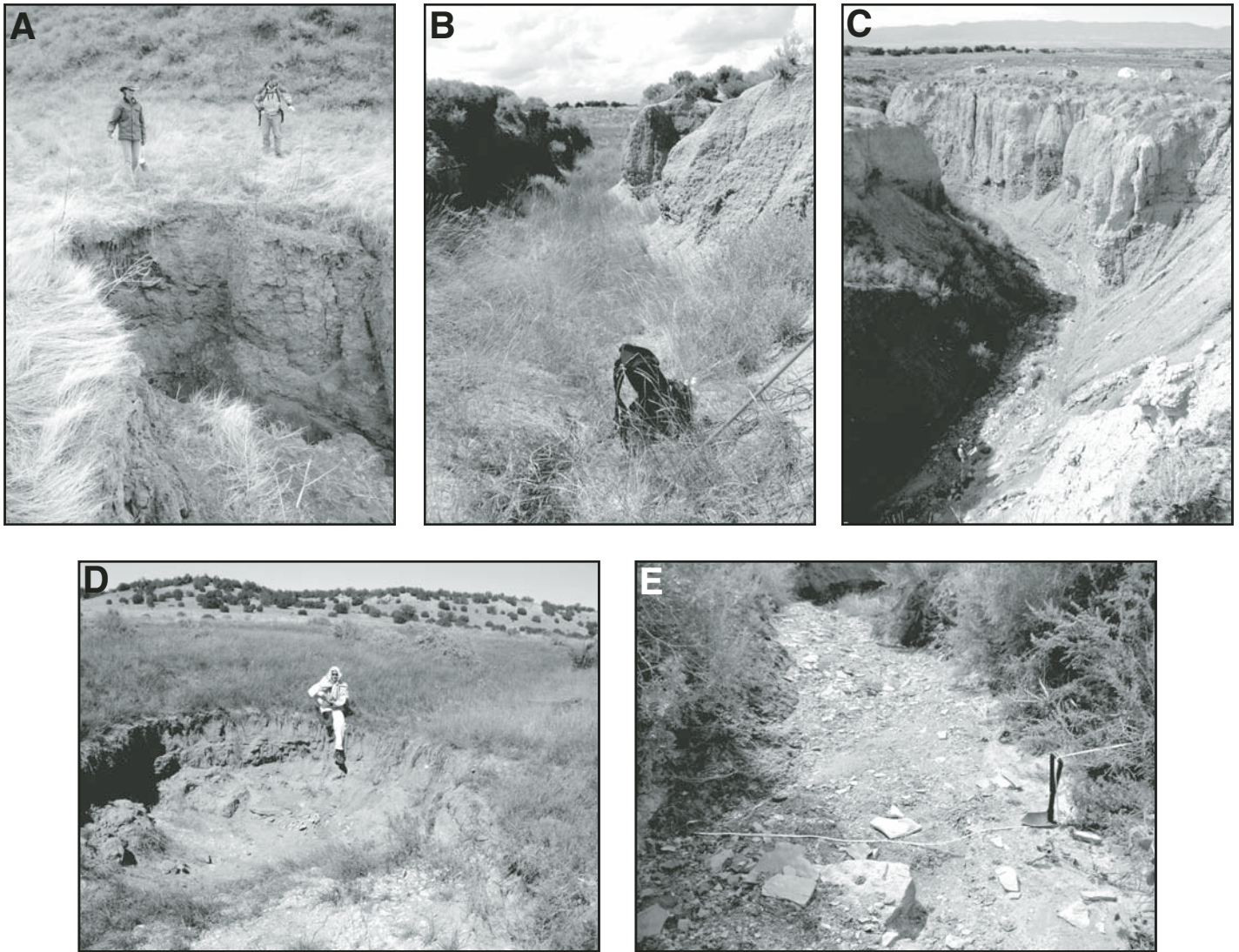


Figure 3. Examples of channels, channel heads, and discontinuous scarp flights. (A) Typical head scarp, West Bijou Creek drainage, central Colorado. The valley above is unchanneled. Note tension crack and incipient slab failure at center right. (B) Grass-lined channel in the Dry Creek drainage basin. Backpack is about half a meter high. (C) Deeply incised, scoured channel in the Red Creek basin. Along the right-hand wall, top center are two large paleochannels, marked by the light-colored fill inset into dark shale bedrock. (D) Head scarp with plunge pool along Big Arroyo (Fig. 1B). Above, the channel consists of a shallow, fully vegetated swale; below is an incised reach that grades downstream into a shallow, overgrown swale before reaching another head scarp. The drainage area here is ~15 km<sup>2</sup>. (E) Close-up view of scoured channel in the Red Creek drainage (same channel as C).

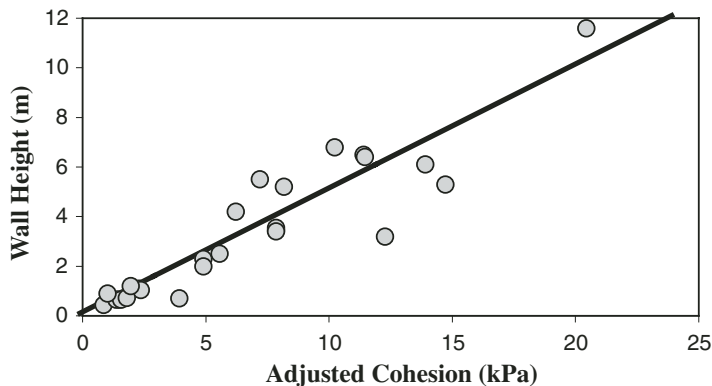


Figure 4. Vertical channel wall height as a function of cohesion (after Istanbuluoglu et al., 2005).

1999 USGS 1:12,000 digital orthophotos. The historic photographs were scanned at high resolution (~30 pixels per meter) and enlarged. All channel heads or prominent in-channel headcuts that were clearly identifiable in both photo series and not obscured by check dams, roads, or other features, were included in the analysis. Given limits in resolution and photograph distortion, the minimum identifiable extent of channel-head advance is on the order of 4–5 m, which represents an average rate of ~6–8 cm/yr. Figure 8 shows an example of two incised channel networks as they were in 1937 and 1999.

The majority of the channel segments analyzed experienced little or no discernible growth over the six-decade period between photo pairs (Fig. 9). The frequency distribution is strongly right-skewed. For example, although most of the networks appear essentially stable; five channel segments (13% of the data set) show average extension rates of more than 45 cm/yr over the 62 yr period between photo pairs. The most rapid average incision rate comes from an ~100-m-long tributary segment, which, by 1999, had incised a previously unchanneled alluvial flat. There is no apparent spatial clustering in the distribution of average extension rates. Given the observations of gully formation dynamics discussed herein, it is likely that the asymmetric spatial distribution of extension rates reflects a combination of varying storm history from site to site and variations in soil properties and land cover.

### Role of Vegetation

The study areas are mantled by grasslands and, to a lesser degree, shrub lands and piñon-juniper woodlands. Grassland cover is known to be highly resistant to overland flow erosion. A common and simple way to describe the erosion resistance of a soil or bedrock is in terms of a threshold shear stress,  $\tau_c$ , below which the rate of material detachment is negligible:

$$D_c \propto \tau^\alpha - \tau_c^\alpha, \quad (1)$$

where  $D_c$  represents the detachment capacity (L/T),  $\tau$  is bed shear stress, and  $\alpha$  is a parameter that depends on the derivation of equation 1 (for example,  $\alpha = 1$  for a linear shear-stress model [Howard and Kerby, 1983] and  $\alpha = 3/2$  for a unit stream-power model [Whipple and Tucker, 1999; Moore and Burch, 1986]). In the presence of vegetation, some portion of the applied fluid shear stress will be expended on plants rather than on the soil directly; this effect is especially pronounced when grasses are flattened by overland flow, forming a barrier between the flow and the soil surface. Shear stress partitioning between plants and soil has been formalized in some models (e.g., Foster, 1982). Here, for consistency with field experiments, we adopt a simpler formalism in which  $\tau_c$  is considered a bulk “effective” value that depends on vegetation cover and encapsulates the degree to which fluid shear is expended on stems, branches, etc., rather than directly on the soil surface. The erosion threshold will also

reflect both intrinsic soil cohesion and effective cohesion imparted by roots.

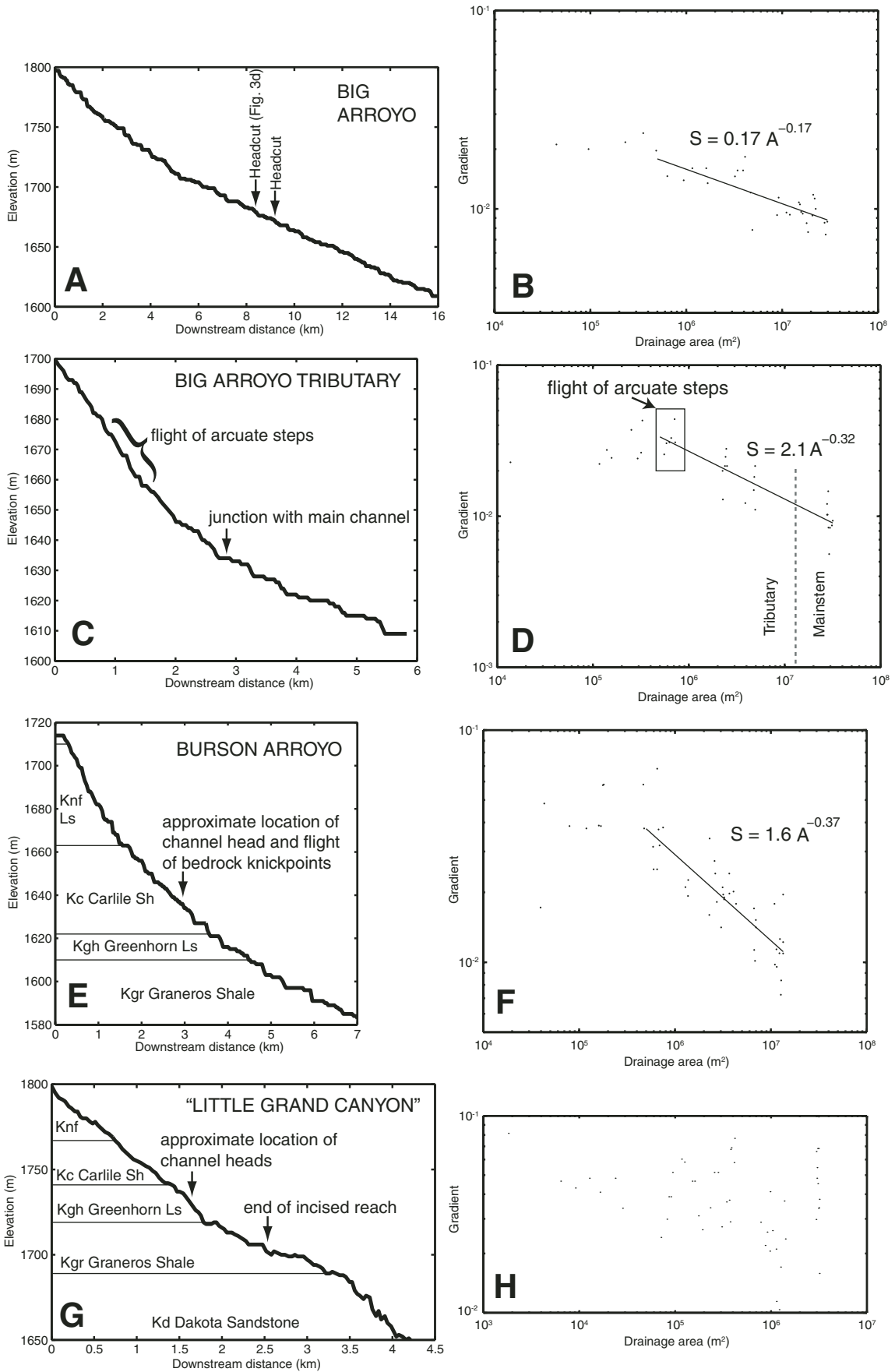
Field studies conducted on grasslands in Australia (Prosser and Slade, 1994) and California (Prosser and Dietrich, 1995; Prosser et al., 1995) suggest that nondegraded grasses and similar herbaceous carpets are able to withstand overland flow shear stresses of a hundred or more pascals without significant erosion (Table 1). Clipping, grazing, and similar damage can apparently reduce this threshold by up to an order of magnitude. The very high resistance of intact herbaceous cover contrasts markedly with bare soils, on which soil detachment and rilling can occur at shear stresses on the order of a few pascals (Table 1).

This hundredfold contrast in erosion threshold between bare soil and full herbaceous cover implies a significant role for vegetation as a mediator of channel formation and development. We have observed a variety of vegetation states in channel floors, ranging from essentially bare to a full cover of herbaceous and woody riparian species (Fig. 3). We have also observed



Figure 5. Example of discontinuous, arcuate steps in an otherwise unchanneled valley tributary to Big Arroyo.

Figure 6. Typical longitudinal arroyo profiles and slope-area trends. (A) Main stem of Big Arroyo, showing location of the channel head shown in Figure 3D, and a second large headcut that marks the upstream termination of another incised reach downstream. (B) Slope-area diagram for the Big Arroyo main stem. Drainage areas in all slope-area plots were mapped using standard digital elevation model (DEM) flow-routing procedures. Gradients were obtained from the DEM by taking the average gradient over a constant vertical drop (in this case, 5 m). (C) Southeastern tributary to Big Arroyo, indicating position of a flight of discontinuous, arcuate steps (pictured in Fig. 5). (D) Slope-area diagram for Big Arroyo tributary. (E) Burson Arroyo, showing the approximate positions of lithologic breaks and the location of the head of the main incised reach, which continues from this point at least as far as the confluence with the main stem of Taylor Arroyo. (The position of the Greenhorn Limestone is only approximately mapped, and may in fact be topographically higher.) (F) Slope-area diagram for Burson Arroyo. (G) Short, deep arroyo (“Little Grand Canyon”) pictured in Figures 3C, 8C, and 8D. Location is indicated by asterisk on Figure 1B. Channel depth is at a maximum at the head (~15 m) and decreases downstream, where it grades into the regional valley slope. (H) Slope-area diagram for the Little Grand Canyon arroyo. Note lithologically related steep reaches on profile and in slope-area data. Profile vertical exaggeration is 50× in A, C, and E, and 20× in G. Lithologies in E and G: Knf—Fort Hayes Limestone member of Niobrara Formation, Kc—Carlisle Shale, Kgh—Greenhorn Limestone, Kgr—Graneros Shale, Kd—Dakota Sandstone.



plants recolonizing channel floors following scour or burial by flash floods. These observations imply a dynamic interaction between flash-flood erosion/deposition and channel-floor vegetation growth (Collins et al., 2004). A sufficiently powerful flash flood can damage or eliminate channel-floor vegetation. The resulting decrease in effective erosion threshold increases the frequency of channel erosion and/or deposition events, which in turn inhibits vegetation growth.

Collins et al. (2004) used a numerical model to examine some geomorphic consequences of this vegetation-erosion interaction. Here, we use a simple, zero-dimensional version of that model (i.e., a single point in a channel) to show how the vegetation state of the channel floor depends on the relative time scales of vegetation growth and flash-flood occurrence, which in turn is a function of climate and drainage-basin scale. The model rules are summarized in Table 2. The state variable,  $V$ , represents the degree of proportional vegetation cover in a single channel reach. The model calculates variations in  $V$  over time in response to a random, exponentially distributed (i.e., Poisson) sequence of flood events. Flood magnitude and duration also follow exponential distributions. When flood discharge exceeds a threshold value that depends on  $V$  (Table 2, rule 1), vegetation is damaged to a degree that depends on excess discharge (over and above the threshold; rule 2) and event duration. Between events, vegetation recovers at a rate that depends on the fraction of vegetation remaining and a specified regrowth time scale (Table 2, rule 3).

Results from three calculations are shown in Figure 10. When floods are rare relative to vegetation regrowth time scales ( $T_g < T_b$ , where  $T_b$  is

average flood recurrence interval), the channel floor remains vegetated except in the immediate aftermath of exceptionally large floods, and there is no correlation between one event and the next (Fig. 10, top). When the flood recurrence interval is short relative to vegetation regrowth time ( $T_g > T_b$ ), the vegetation remains sparse because it is frequently disturbed (Fig. 10, bottom) (such a cover might correspond to a thin carpet of young, fast-growing annuals and seedlings of slower-growing species, with seed stock provided from surrounding banks and hillslopes). Between these end cases, there is an interesting realm of behavior in which flood recurrence interval is comparable to vegetation regrowth time (Fig. 10, center). When  $T_g \geq T_b$ , the effectiveness of any given flood varies considerably, depending on the antecedent history of erosion and vegetation growth. Autocorrelation analysis reveals that when  $T_g \geq T_b$ , the modeled vegetation time series are autocorrelated on a time scale comparable to the regrowth time.

The ratio  $T_g/T_b$  will depend on several factors, including climate, soil moisture, vegetation type, soil physical properties, and catchment scale. In the southern study area, experience with vegetation restoration suggests that locally disturbed grassland can reach near-full recovery in about three years when reseeded, watered, and covered (B. Miller, 2002, personal commun.). This represents an  $e$ -folding time scale ( $T_g$ ) on the order of one year, which is a minimum regrowth time: natural regrowth presumably can take longer, depending on the history of rainfall and soil moisture following disturbance. It is reasonable to suppose that vegetation properties and regrowth time  $T_g$  will vary somewhat between an open, unchanneled valley floor, and an incised channel floor. In the study region,

incised channels tend to host more woody species (e.g., the invasive exotic *Tamarix*) relative to grasses, and contain higher soil moisture. Such effects are obviously not incorporated in the simple model summarized in Table 2. It would be interesting to discover the extent to which the interaction of soil moisture, topography, and species competition influences geomorphic behavior. This could be done with a combination of monitoring of vegetation type and density and greater attention to the role of soil moisture and plant species composition in an improved erosion-hydrology-vegetation model.

Vegetation regrowth time can be compared with flash-flood recurrence interval, which varies significantly with both climate and basin size. Table 3 shows a sample of recurrence-interval estimates for flash floods in ephemeral basins smaller than 150 km<sup>2</sup> in south-central Colorado. These are generally shorter than the time scale for vegetation regrowth, though it is likely that the recurrence interval for erosionally effective events is larger, perhaps on the order of regrowth time. These data indicate that ephemeral channels in the study area tend to lie in the realm of behavior corresponding to  $T_g/T_b \geq 1$  (Fig. 10, middle and bottom).

The foregoing observations and analysis indicate that the role of vegetation in arroyo dynamics varies systematically with basin scale, among other factors. Because of the surprisingly high erosional resistance of grassland vegetation, channel initiation in semiarid grasslands is likely to require either very intense storms or significant degradation of the vegetation armor. In the next section, we examine, via two case studies, the necessary conditions for generating sufficiently high shear stresses to penetrate an intact turf cover.

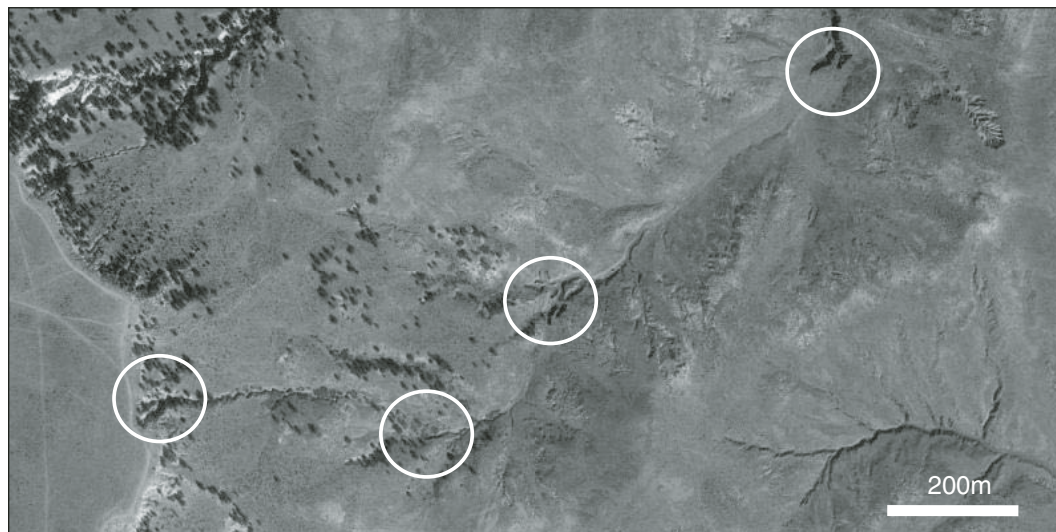


**Figure 7.** Example of multiple, discontinuous channel segments along a drainage, West Bijou Creek basin, Colorado. Circles show the positions of active channel heads (source: U.S. Geological Survey digital orthophoto, 1999; latitude 39.458°N, longitude 104.327°W).

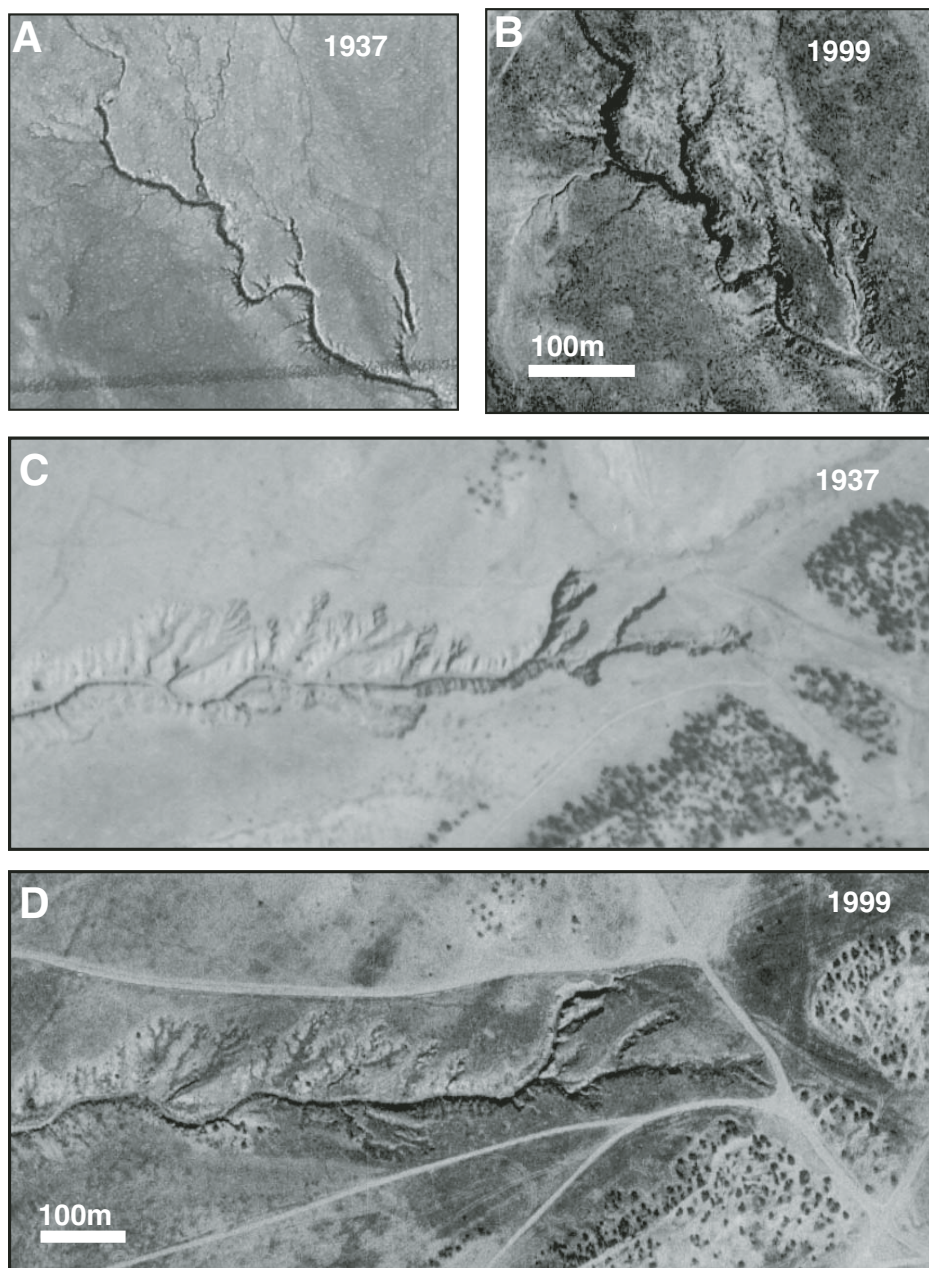


**Figure 8.** Aerial photographs of two arroyo networks in 1937 and 1999. (A, B) Network in the Dry Creek drainage basin (latitude 38.447°N, longitude 104.697°W). (C, D) Network in the Red Creek drainage basin (location shown by asterisk on Fig. 1B; latitude 38.467°N, longitude 104.935°W; see also Figs. 3C, 6G, and 6H).

## HYDROLOGY AND FLASH-FLOOD DISCHARGE RECONSTRUCTION

### Runoff Generation

Observations at the study sites indicate that rainfall generated by summer convective storms can generate large volumes of infiltration-excess overland flow within the storm core (Fig. 11). Because the water table in the study sites is nor-

mally tens of meters below the ground surface (von Guerard et al., 1987), saturation-excess overland flow is likely to be rare.

Measurements of soil infiltration capacity were obtained using a Guelph permeameter at several locations within the study area (Table 4). These point-estimates of final infiltration capacity range widely, from <1 to ~300 mm/h, with mean values by site on the order of a few tens to ~100 mm/h. By comparison, inspection

of USGS 2004 peak rainfall and runoff data for three ephemeral tributaries of the Purgatoire (Bent Canyon Creek, Lockwood Arroyo, and Taylor Arroyo) shows that storms with a peak 5 min intensity as high as several tens of mm/h and total rainfall depths of 1–2 cm measured at a stream gauging station can nonetheless fail to generate measurable flow. Thus, although we do not have very good estimates of effective infiltration and interception capacities at scales comparable to the width of a convective cell's core (say, hundreds of meters to a few kilometers), flash-flood generation in the study area is likely to require peak rainfall intensities of a few tens of mm/h at a minimum.

### Case Studies of Flash-Flood Occurrence

Given that grassland vegetation imposes a significant threshold for runoff erosion—up to two orders of magnitude higher than that for bare soil—it is important to consider under what conditions runoff of sufficient magnitude can be generated. If, given the topography of the region, flow events capable of generating hundreds of pascals of bed shear stress are common, then it is likely that arroyo initiation in the region would also be common under modern climate conditions, even in the absence of land disturbance. On the other hand, if the recurrence interval of events large enough to cut channels is comparable to or greater than the time scale of significant climate shifts, major droughts, and/or vegetation changes ( $10^3$ – $10^4$  yr), this would suggest that some form of disturbance is needed for the formation of widespread channel networks under modern climate conditions. To some extent, this is a question of basin scale. In this section, we examine documented examples of flash-flood occurrence.

An intense convective storm struck a group of small watersheds in the Sullivan Park area of the Red Creek basin (Fig. 1B) in August 1999. A second one hit the same area on 13 July 2001. Both events caused check dams to overflow, and the spillways of at least two of these dams were heavily damaged (Fig. 12). The first event was sufficient to cut through the turf mat lining the spillway and carve a channel ~4 m deep and ~7 m wide (Fig. 12A).

Between the two events, the spillways had been lined with geotextile and armored with ~21-cm-diameter granite boulders. During the 2001 event, at one location, the boulder armor and geotextile were completely undermined and eroded. At a second location, the armor was stripped off only from the steepest portion of the spillway; it remained intact on the lower-gradient upper portion (Fig. 12B). Observation

of flood marks along the throat of one spillway immediately after the 2001 event (J. Kulbeth, 2001, personal commun.) allows estimates to be made of peak discharge and runoff intensity. The gradient along the spillway was measured using a hand level, which is accurate to about ± 0.5 degrees. Spillway throat dimensions were provided by J. Kulbeth. The mean flow velocity,  $\bar{U}$ , and peak discharge,  $Q_p$ , at the spillway throat were estimated using the Law of the Wall for fully turbulent flow:

$$Q_p = \bar{U}A = \frac{AU_*}{\kappa H} \int_{z_0}^H \left(\frac{z}{z_0}\right) dz, \quad (2)$$

where  $A$  is channel cross-sectional area,  $\kappa$  is von Kármán's constant,  $H$  is flow depth,  $U_* = \sqrt{gRS}$  is shear velocity,  $g$  is gravitational acceleration,  $R$  is hydraulic radius,  $S$  is gradient,  $z$  is height above the bed, and  $z_0$  is roughness length. Measured bed slope was used as an estimate of hydraulic gradient, and  $z_0$  was taken to be 1/30th of the boulder diameter. Allowing up to 50% error in hydraulic gradient (i.e.,  $1 \pm 0.5^\circ$ ), the estimated peak discharge ranges from 9 to 16 cm (Table 5). This corresponds to a peak effective runoff rate, averaged over the ~0.5 km<sup>2</sup> catchment, of 65–113 mm/h. By comparison, a tipping-bucket rain gauge ~1 mile to the north recorded a peak 5 min rainfall intensity of 78 mm/h. The low end of the runoff estimates is comparable to measured peak rainfall and allows a plausible ~10 mm/h infiltration rate. The upper end requires rainfall to have been several tens of mm/h higher over the catchment than at the rain gauge; given the small radius and high spatial variability typical of thunderstorm cells, this is also plausible.

The estimated peak shear stress at the spillway throat falls in the range 40–130 Pa. The equivalent shear stress at the steepest (5°) portion of the spillway channel was estimated using the Manning equation with roughness coefficient  $n = 0.033$ , which most closely matches the previous Law of the Wall calculation. For a 5° gradient, the estimated peak shear stress is just short of 300 Pa. By comparison, the critical shear stress for entrainment of 21 cm boulders on a uniform bed (as this was) ranges from ~100–200 Pa for critical Shields stress values of 0.03–0.06 (cf. Buffington and Montgomery, 1997). Thus, our discharge and shear stress estimates are consistent with the fact that boulders were entrained and removed only on the steeper section of the channel.

These two case studies provide an example of the dramatic form and magnitude of incision that can occur when the vegetation armor (or, in the case of the 2001 event, artificial cover)

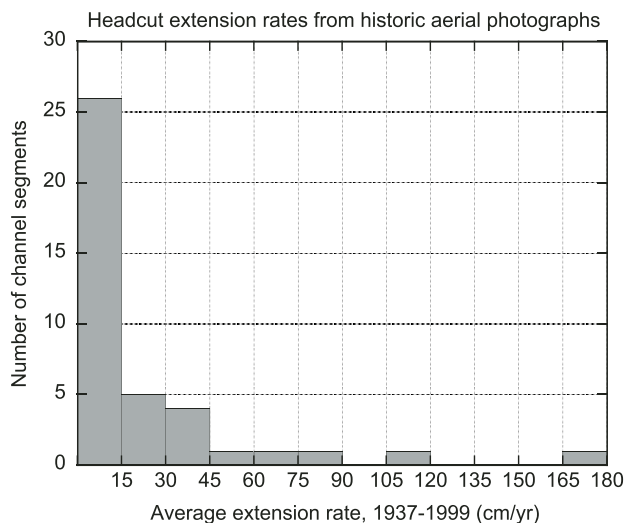


**Figure 9. Rates of channel headcut extension estimated from 1937 U.S. Department of Agriculture (USDA) (1:20,000) and 1999 U.S. Geological Survey (1:12,000) aerial photographs. First column includes channel segments for which the extension rate was indistinguishable from zero. Estimated precision of the method is about ±6–8 cm/yr.**

TABLE 1. ESTIMATED EROSION THRESHOLDS FOR BARE AND GRASS-COVERED SOIL

Condition	Estimated threshold shear stress (Pa)	Source
Bare agricultural soil	3.1 ± 1.8†	Elliott et al. (1989)
Bare agricultural soil	1.7–10.6	Gilley et al. (1993)
Bare, poorly cohesive soils	0.6–4.4	(see note †)
Bare clay	21	Reid (1989)
Clipped bunch and sod grass	20–40 (>70–80)*	Prosser and Dietrich (1995)
Lightly disturbed tussock grass and sedge	>180	Prosser and Slade (1994)§
Bunch and sod grass	100–180 (>150–230)#	Prosser and Dietrich (1995)
Grass and sedge	> 240	Prosser and Slade (1994)§
Grass	>80–200	Reid (1989)††

†Mean and standard deviation from 32 soil-plot experiments on different soils; each data point represents an average of six runs at the same site.

‡Data compiled by Prosser and Dietrich (1995) from Crouch and Novruzi (1989), Slattery and Bryan (1992), and Merz and Bryan (1993).

§Prosser and Slade (1994) found that flows generating basal shear stresses between 160 and 330 Pa were unable to cause incision in a cover of dense grass and sedge; when the cover was lightly disturbed, flows greater than 180 Pa caused patchy scour without incision.

\*The first values represent thresholds for sediment transport, while those in parentheses indicate minimum thresholds for incision into the vegetation mat, which Prosser and Dietrich (1995) estimated as at least 50–60 Pa higher than the sediment-transport threshold.

††Reid's (1989) estimate combines Ree's (1949) estimates of nonerosive flow velocities with velocity-stress relation. They are thus minimum estimates for  $\tau_c$ .

TABLE 2. VEGETATION GROWTH-EROSION MODEL FOR EPHEMERAL CHANNEL FLOORS

Governing equations	Symbols
1. VEGETATION INCREASES EROSIONAL RESISTANCE $\hat{H}_c = \hat{H}_{cs} + \hat{H}_{cv}V$	$V$ = Proportional surface vegetation cover $\hat{H}$ = Flood depth (stress per unit water weight per unit hydraulic gradient) normalized by threshold depth for $V = 1$
2. VEGETATION IS DAMAGED BY EROSIONAL FLOODS $\frac{dV}{dt} \Big _{\text{erosion}} = -\frac{EV}{L_r} = -\frac{(\hat{H} - V)V}{T_c}$	$\hat{H}_t$ = Threshold flood depth relative to maximum threshold at $V = 1$ $\hat{H}_{cs}, \hat{H}_{cv}$ = Proportion of erosion threshold due to soil cohesion and vegetation resistance, respectively, at $V = 1$
3. VEGETATION GROWS BACK BETWEEN FLOODS $\frac{dV}{dt} \Big _{\text{growth}} = \frac{1 - V}{T_g}$	$t$ = Time $E$ = Vertical erosion/sedimentation rate [L/T] $L_r$ = Characteristic root depth [L] $T_c$ = Time scale for vegetation erosion/damage $T_g$ = Time scale for vegetation regrowth

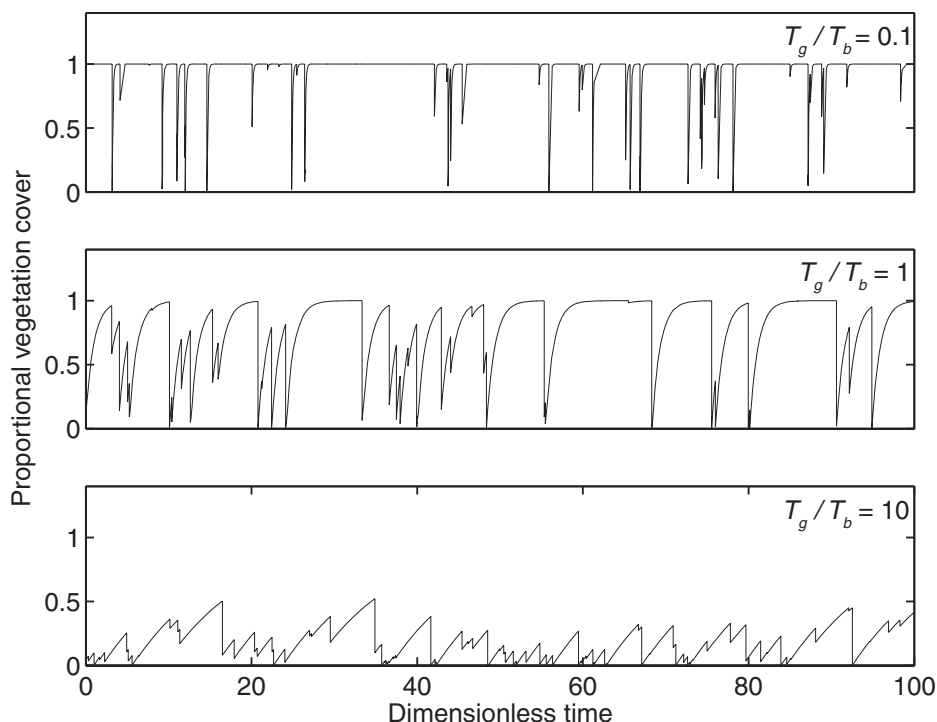


**Figure 10.** Time evolution of channel-floor vegetation cover computed using the model in Table 2. The three graphs compare solutions with different ratios of vegetation regrowth time scale ( $T_g$ ) to average storm return period ( $T_b$ ). Other parameters are:  $H_{cv} = 1$ ,  $T_r/T_b = 0.05$ ,  $T_r/T_b = 0.01$ , and  $\langle H \rangle/H_{c0}$ , where  $T_r$  is mean flood duration,  $\langle H \rangle$  is mean flood depth,  $H_{c0}$  is minimum flood depth (shear stress per unit downslope water weight) for erosion, and the other parameters are as defined in Table 2.

is penetrated. It is worth asking: what is the typical recurrence interval for a gully-forming event in an unchanneled valley (or, as is common in basins of several km<sup>2</sup> or larger, a valley containing a shallow and fully carpeted swale-like channel form that lacks sharp banks)? The estimated recurrence intervals for the 1999 and 2001 Sullivan Park storms, recorded at a station ~1 mile from the erosion site, are listed in Table 5. The recorded peak rainfall intensity for both events has an estimated return period of 1–3 yr based on the NOAA Atlas 2 database (Miller et al., 1973; Arkell and Richards, 1986). Thus, these two channel-forming events were reasonably common, and they suggest that localized convective storms can, with reasonable frequency, generate Hortonian runoff with short-term peak runoff rates of several tens to possibly over 100 mm/h in small (order 1 km<sup>2</sup>) basins. However, because gully formation occurred in the spillways of check dams, where the gradient is significantly steeper than the valley gradient, the recurrence interval for the Sullivan Park events is not necessarily indicative of the frequency of gully-forming events in natural valleys.

### Peak Discharge Reconstruction in Existing Arroyo Networks

Because rangeland vegetation is such an effective barrier to runoff erosion, it is also worth asking: what are typical recurrence intervals for flash floods in small basins (~0.5–15 km<sup>2</sup>)? This is not easy to determine without gauging data, which do not exist in our study areas for basins smaller than 40 km<sup>2</sup>. However, estimates can be obtained by combining rain gauge data with estimates of peak discharge obtained from flood debris. To that end, we measured high-water marks, channel cross sections, and channel gradients along reaches of two arroyos that conveyed flash floods in August 2003 (Fig. 2). Using the Law of the Wall method (equation 2) to estimate flow velocity and discharge, the estimated peak discharge, based on three cross sections, was on the order of 3–4 m<sup>3</sup>/s along the lower reach of Burson Arroyo (drainage area ~7 km<sup>2</sup>; see Fig. 1C). A central reach of Big Arroyo, which is both larger (drainage area ~15 km<sup>2</sup>) and appears to have been closer to the storm core (Fig. 2), had a peak discharge on the order of 50–60 m<sup>3</sup>/s.

**TABLE 3.** RECURRENCE INTERVALS FOR FLASH FLOODS IN EPHEMERAL BASINS <150 km<sup>2</sup> IN SOUTH-CENTRAL COLORADO

Basin	Drainage area (km <sup>2</sup> )	Recurrence interval (yr)
Big Arroyo	40	0.20
Burke Arroyo tributary	12	0.56
Taylor Arroyo	125	0.15
Red Rock Canyon Creek	126	0.41
Bent Canyon Creek	146	0.47
Lockwood Canyon Creek	127	0.11

*Note:* Data are from U.S. Geological Survey. For purposes of calculating recurrence interval, an event is defined as a daily flow that exceeds the flow on both previous and subsequent days.

The floods were triggered by a thunderstorm with a peak 15 min rainfall intensity of 86 mm/h recorded at a rain gauge located ~1.5 km and 3.5 km from the Big Arroyo and Burson Arroyo sites, respectively (Fig. 2). This rainfall intensity has a 3 yr recurrence interval (Table 5). In Burson Arroyo, the flood produced an estimated cross-section-averaged shear stress of 40–50 Pa, and a peak (thalweg) shear stress of 50–90 Pa. These shear stresses fall below the estimated minimum vegetation-undermining stress in Table 1, and indeed evidence of scour was limited to occasional patches along the channel thalweg. Based on three cross sections, the larger flood in Big Arroyo produced cross-section-averaged shear stresses on the order of 85 Pa in two sections with gradients typical of this stretch of the valley (~0.013), and ~170 Pa in a locally steeper (slope = 0.03) section. Corresponding estimated peak thalweg shear stresses are ~130 and ~350 Pa, respectively. Thus, this roughly 3 yr event produced peak shear stresses that begin to approach, and locally exceed, the minimum threshold for undermining an intact turf mat. These estimates are consistent with an observed pattern of localized intense scour around knickpoints but limited channel incision elsewhere, as discussed below.

Next, we briefly consider the extent to which a 100 yr flood might be capable of driving large-scale channel incision in the study areas. Let us assume, for the sake of argument, that flood magnitude scales with recurrence interval in the same way that rainfall magnitude does—that is, for example,  $Q_{100}/Q_2 = P_{100}/P_2$ . This probably underestimates flood magnitude, given likely nonlinearities in rainfall-runoff transformation, but is about the best we can hope for, given the uncertainties. Based on this, a rough estimate of the equivalent 100 yr flood in the studied reach of Big Arroyo is ~120 m<sup>3</sup>/s. Calculating the likely impact of such an event using the same three cross sections in Big Arroyo reveals

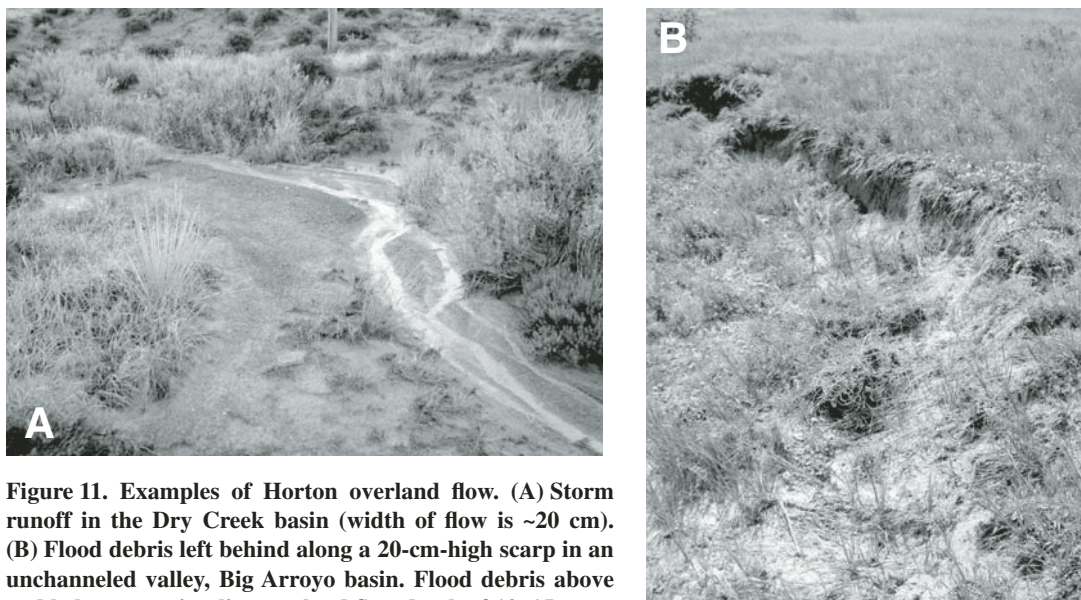


**Figure 11.** Examples of Horton overland flow. (A) Storm runoff in the Dry Creek basin (width of flow is ~20 cm). (B) Flood debris left behind along a 20-cm-high scarp in an unchanneled valley, Big Arroyo basin. Flood debris above and below scarp implies overland flow depth of 10–15 cm.

the critical role played by locally constricted and oversteepened reaches. The role of channel constriction can be appreciated by comparing the impact on representative incised versus unincised sections (Fig. 13). Assuming for the moment that the gradient is the same in both reaches (equal to the reach average channel gradient of 0.013), we find that our estimated 100 yr event produces a 73% higher section-averaged shear stress in the incised channel as compared to the unincised valley floor upstream (Figs. 13A and 13B). The incised reach also happens to be steeper by a factor of >2 relative to the average valley gradient. Accounting for this oversteepening (Fig. 13C), peak shear stress in the incised reach is nearly twice as large as it would otherwise be; in this case, the estimated 100 yr mean and peak stresses both exceed the estimated threshold for ripping out the turf cover (Table 1).

This example illustrates the importance of local channel slope and constriction in generating shear stresses sufficient to drive significant erosion during flash floods. What does it mean for channel form and dynamics? A common channel pattern in the study area is the presence of stretches of incised channel with an active headcut and plunge pool, or sequence of these, at the upstream end (Figs. 3A, 3D, and 7). Above this, there is usually a nonincised valley segment that is either completely unchanneled (common in basins on the order of 1 km<sup>2</sup> or less) or contains a shallow and subtle channel form that is completely mantled by vegetation (e.g., basins on the order of several tens of km<sup>2</sup>) (Fig. 7). Next, we interpret this pattern in terms of hydraulic force and erosional susceptibility.

## DISCUSSION AND CONCLUSIONS

### Form and Dynamics

The foregoing observations provide a picture of the dynamics of these ephemeral channel networks and lead to the following interpretation. Consider an unchanneled, grass-carpeted rangeland valley floor underlain by cohesive alluvium and/or friable bedrock. Based on the field studies listed in Table 1, the vegetation carpet will have an effective erosion threshold comparable to that of decimeter-scale boulders, while the threshold for eroding the underlying material is up to two orders of magnitude lower (Table 1). Thus, the valley floor is conditionally unstable, in the sense that any local perturbation sufficient to break through the vegetation armor will tend to grow by positive feedback. As the depth of erosion increases and root density decreases, the substrate will tend to weaken, and the gradient above the growing scour will grow, possibly forming a “shock” with a vertical scarp and plunge pool (Figs. 3, 5, and 11B). However, there are several negative feedback mechanisms that prevent runaway growth. Scour depth will be limited by the need to maintain a downslope hydraulic gradient sufficient to transport eroded material. If a plunge pool forms, its depth will be limited by subaqueous diffusion of the incoming turbulent jet (e.g., Stein et al., 1993). Headward retreat of the growing scarp will also inhibit concentrated deepening in one spot. The importance of headward retreat as a negative feedback to local deepening is supported by the observation that the deepest head scarps tend to

form where headward retreat is inhibited, for example, by an outcrop of locally resistant bedrock (Fig. 3C) or by tree roots. In addition, the short duration of flash floods limits the depth of scour during a single event. Finally, any lateral widening immediately below a head scarp can lead to reduction in mean and maximum bed shear stress.

The latter negative feedback also illustrates the important role of substrate cohesion. In noncohesive sediment, rapid and efficient channel widening would act as a powerful negative feedback against focused scour. Istanbuloglu et al. (2005) provided numerical examples of how low cohesion is associated with significant gully-head widening, and vice versa. Thus, a cohesive substrate is a necessary, though not sufficient, condition for the observed morphology and dynamics of incised arroyos.

Sediment concentration is another factor that promotes focusing of erosion around a retreating head scarp. A flash flood moving along an

**TABLE 4.** HYDRAULIC CONDUCTIVITY AND GRAIN SIZE OF SURFACE SOILS

Site	$D_{50}$ (mm)	Field-saturated hydraulic conductivity (cm/hr)
HRT	0.028 ± 0.025 (n = 9)	10.3 ± 5.2 (n = 5)
BV	0.046 ± 0.069 (n = 6)	4.1 ± 2.4 (n = 2)
LGC	0.012 ± 0.012 (n = 6)	2.2 ± 2.0 (n = 5)
BA1	0.016 ± 0.022 (n = 7)	6.4 ± 10.8 (n = 7)
BA2	0.044 ± 0.029 (n = 5)	4.5 ± 2.5 (n = 4)
LW	0.054 ± 0.069 (n = 8)	11.7 ± 10.2 (n = 6)

*Note:* Table shows mean and standard deviation. Data are from Flores (2004).

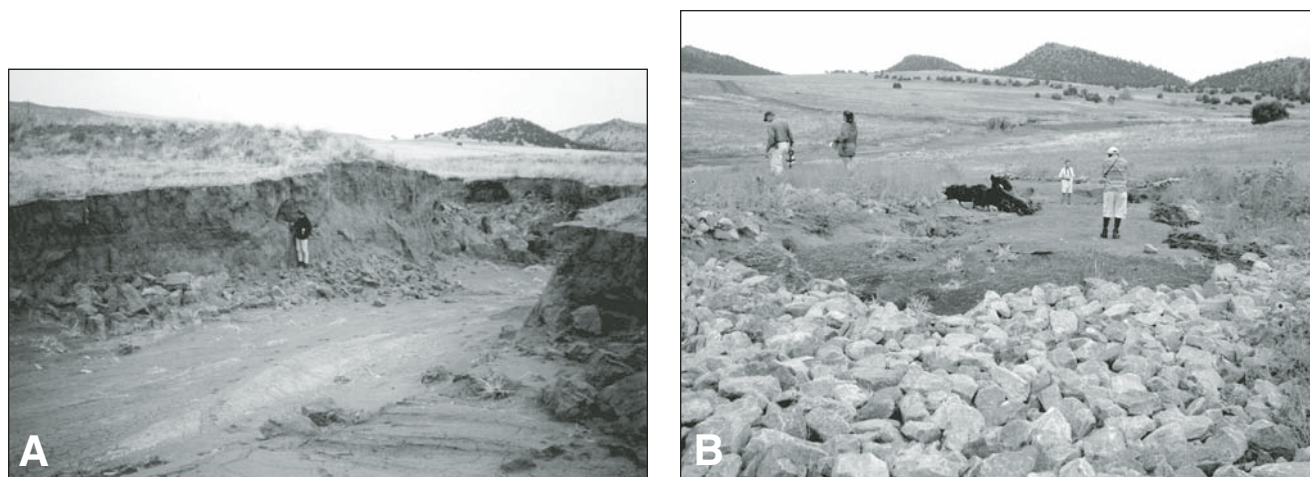


**Figure 12.** (A) Gully carved in check-dam spillway by convective storm in August 1999. The spillways had recently been worked on, so that the turf mat was weaker than a mature cover (B. Goss, 2005, personal commun.). (B) Damage to a boulder- and geotextile-lined spillway by convective storm on 13 July 2001.

unchanneled valley segment will tend to have negligible bedload concentration, because any coarse sediment entrained from an upstream incised segment will tend to come to rest near or above the termination of the channelized reach, where channel widening leads to a reduction in boundary shear stress. Thus, flow entering the head of an incised reach will tend to have a high transport capacity for coarse sediment. Sediment concentration will rapidly increase where the flow crosses an actively eroding/retreating head scarp, and the resultant reduction in excess transport capacity—together with downstream channel widening and the consequent reduction in boundary shear stress—will further inhibit scour downstream. This interpretation is supported by the observation in our study areas that gravel bars containing locally derived sediment commonly drape the channel bed within meters to tens of meters below an active scarp or channel head.

This conceptual model suggests the following necessary and sufficient conditions for the formation of incised ephemeral channels containing one or more headward-propagating segments. A resistant surface layer overlying a weaker substrate sets up an instability in which erosional perturbations can grow by positive feedback. High flow variability (e.g., an ephemeral channel subject to occasional flash floods)

allows for vegetation growth between flood events, while providing erosive floods with great enough frequency to maintain a valley form. Moderate to high substrate cohesion (on the order of several kPa or higher; Istanbuloglu et al., 2005) is necessary to prevent a growing erosional perturbation from being rapidly dissipated by bank collapse and channel widening. A high volume fraction of fine-grained material allows for significant, long-distance removal of sediment away from the zone of focused erosion (Kirkby and Bull, 2000), while the presence of a minor but not negligible coarse (bedload) fraction tends to inhibit further sediment entrainment and channel incision downstream of an active headcut.

#### Role of Convective Storms and Implications for Long-Profile Evolution

Our observations of recent flash-flood events show that despite the low relief and gentle valley gradients in the study areas, convective summer storms are able to generate tens to hundreds of pascals of shear stress, depending on channel or valley morphology and local gradient. In locally steep and/or constricted channel reaches, fairly common (3–5 yr) events appear to be able to locally exceed the significant erosion thresholds

associated with grassland vegetation (~200–300 Pa; Table 1). On the other hand, the analysis in Figure 13 suggests that even very large and rare (100 yr) events are generally incapable of generating widespread incision of open, essentially unchanneled valley segments. Thus, valley incision appears to be driven primarily by episodic retreat of channel heads and within-channel knickpoints.

The limited footprint of most convective storms has important implications for the style of valley evolution. The core of a convective cell may cover only several square kilometers (Fig. 2; Goodrich et al., 1997; Bull et al., 1999). Below their source area in the storm core, flash floods will also attenuate due to in-stream infiltration; for example, the Big Arroyo flash flood of 2003, which produced an estimated peak flow of 50 m<sup>3</sup>/s of rainfall in its middle reaches (see rainfall pattern in Fig. 2), generated a peak flow of less than 1 m<sup>3</sup>/s at the catchment outlet (D. Sharps, 2003, personal commun.). Thus, the common assumption in landscape evolution models that channel-forming discharge is proportional to basin area is inapplicable in this type of setting. However, although flood magnitude will tend to diminish rather than increase downstream (outside of the storm core), flood frequency will still increase with basin area. This downstream increase in flood frequency is a likely explanation for the upward concavity of channel profiles (Fig. 6), for the following reason: Over time, and in the absence of strong local forcing (e.g., an active fault), there is a natural tendency for the long-term rate of incision to equilibrate along a channel network (e.g., Hack, 1960; Snow and Slingerland, 1986; Willgoose, 1994). In a convective-dominated

TABLE 5. ESTIMATED RECURRENCE INTERVALS OF FLASH FLOODS, 1999–2003

Location	Date	Peak rainfall rate (mm/hr):			Recurrence interval (yr)
		15 min	30 min	60 min	
Sullivan Park	4 August 1999	61	42	22	1.3 / 1.3 / 1.1
Sullivan Park	13 July 2001	78	60	34	2.3 / 3.4 / 2.8
Burson Well	8 August 2003	86	70	36	3.1 / 5.0 / 3.3

climate like that of the high plains, higher-order valley segments experience more frequent flash floods than lower-order ones. If denudation rates are similar throughout a given network, then greater flood frequency in the higher-order branches must be balanced by reduced average flood effectiveness. Downstream reduction in gradient ensures this. Thus, we interpret the concave-upward valley profiles in our study area as a delicate adjustment between flood frequency and valley gradient, which controls average flood effectiveness. Erosional “punches,” according to this interpretation, become stronger but less frequent with decreasing basin size. A corollary is that time-variability in sediment yield will tend to decrease systematically with basin size, a behavior that appears generally applicable to fluvial systems (e.g., Farnsworth and Milliman, 2003).

Our findings also support the view that relatively small variations in valley gradient can have a large impact on susceptibility to channel incision (e.g., Patton and Schumm, 1975; Dietrich et al., 1993; Bull, 1997). This sensitivity is a direct reflection of the nonlinear relation between boundary shear stress and erosion rate (represented here by an erosion threshold).

#### Scaling Analysis of Long-Profile Concavity

Is a balance between flash-flood frequency and geomorphic effectiveness a plausible explanation for long-profile concavity in this field setting? The following is a brief justification based on scaling arguments. We wish to examine the relative importance of valley slope versus basin size in controlling the average rate of geomorphic work. A simple way to describe the average rate of geomorphic work done by flash floods is  $P = FM$ , where  $P$  represents the average rate of work per unit channel length,  $F$  is the frequency of flash floods ( $T^{-1}$ ), and  $M$  is the average work per unit channel length performed by a single flood (which might be taken to scale with the product of event duration and stream power per unit channel length). (Note that work, in the mechanical sense, is only one possible measure of geomorphic effectiveness; but it is adequate for this demonstration.) The goal is to estimate how  $F$  and  $M$  will vary with basin area and gradient, and whether it is reasonable to expect a balance between these two quantities given the characteristic topography in our study areas.

Consider a dryland catchment in which the predominant rainfall events have a small footprint relative to basin size. Assume that the events are short enough such that, beyond a relatively small length scale ( $10^1$ – $10^2$  m), peak discharge and flood duration are roughly independent of

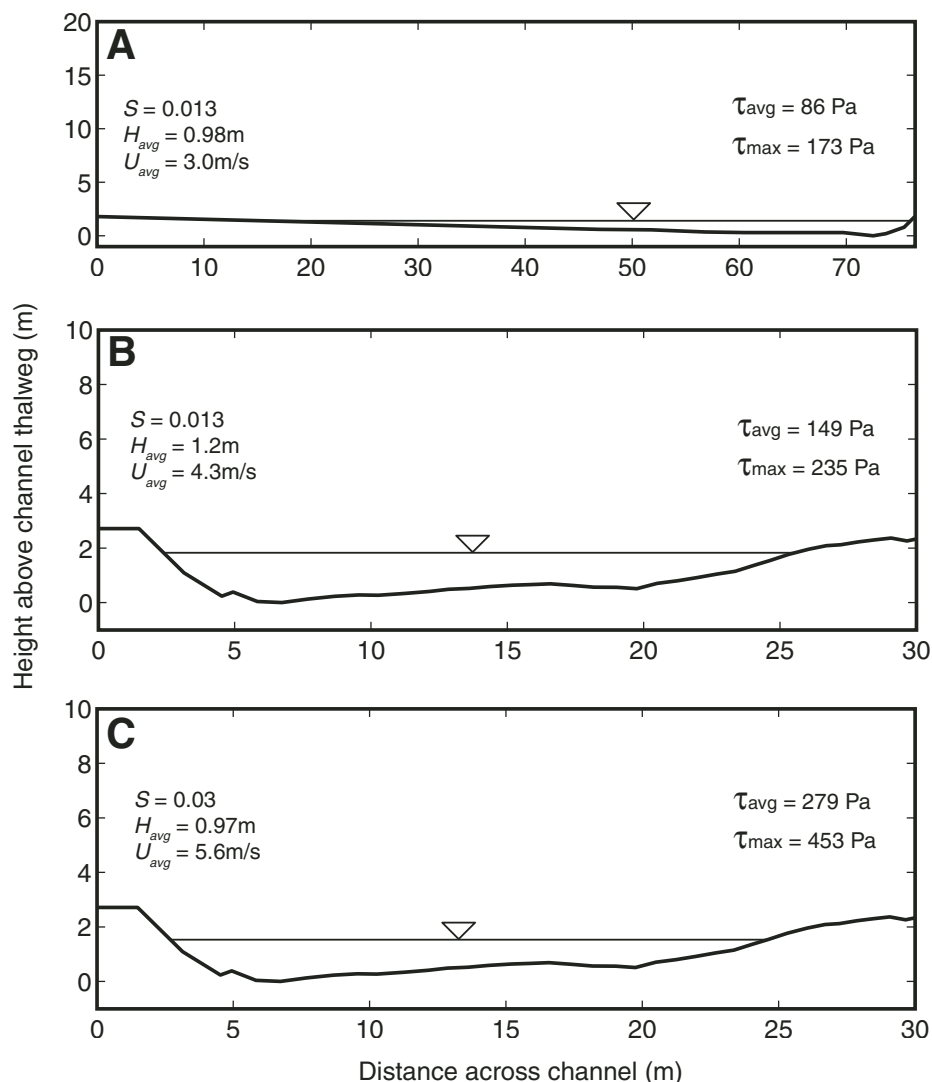


**Figure 13.** Cross sections in the central reach of Big Arroyo, showing calculated 100 yr flood inundation; there is no vertical exaggeration (but note scale difference in top figure). (A) Shallow, fully vegetation-draped upstream section. (B) Downstream section, with flow parameters calculated using the same reach average valley gradient as in A. Increased shear stress relative to upstream section is solely due to channel constriction. (C) Same as B but using local channel gradient of 0.03.

drainage area. Implicit here is the assumption that in-stream losses are small; although this is not necessarily true of typical dryland streams, one might imagine that, on average, in-stream losses (leading to downstream reduction in discharge) might be roughly compensated by a tendency toward increasing runoff downstream even for small-footprint convective storms. If the at-a-point storm arrival rate is homogeneous (that is, the average arrival rate at a point is the same across the basin), then the total storm arrival rate, and thus flood frequency, for the catchment as a whole will be proportional to drainage area. Thus, we can express flood frequency as  $F = bA$ ,

where  $A$  is basin area and  $b$  is the arrival rate of flood-producing storms per unit area.

The average effectiveness of a given flood discharge  $Q$ , in terms of potential geomorphic work, will depend on a variety of factors, including slope, valley/channel geometry, substrate (rock or sediment) properties, and surface roughness. Let us suppose, however, that all of these effects except slope are similar throughout the network. To what extent does the average erosional work performed by a flash flood depend on slope? This issue is a matter of some debate—different erosion models have different implications—but for our purposes, the important

thing is that, due to the presence of an erosion threshold, the relationship is both positive and nonlinear: doubling the channel or valley slope will tend to produce more than twice the erosive potential (e.g., Tucker, 2004). A simple way to approximate such nonlinearity is with a power law:  $M = cS^d$ , where  $S$  is valley or channel gradient,  $d$  is an exponent  $>1$ , and  $c$  is the average work done at unit gradient. This power law is a purely heuristic device designed to capture the fact that an increase in gradient both increases the erosive potential of a given flood (all else equal) and increases the fraction of floods that generate boundary shear stresses sufficiently high to cross the resistance threshold. Based on the arguments advanced in several recent papers (Snyder et al., 2003; Tucker, 2004; Lague et al., 2005; Molnar et al., 2006), the value of  $d$  that best approximates the threshold effect will vary according to the strength of the threshold relative to a characteristic shear stress; as an example, data on gradient versus incision rate from a set of catchments along the northern California coast can be fit with  $d \approx 4$  (Snyder et al., 2003), though this number is surely not universal. Using this device, our average rate of work is:

$$W = bcAS^d. \quad (3)$$

In order for the average rate of work to be the same throughout a valley network, it must be true that

$$S \propto A^{-1/d} = A^{-\theta}. \quad (4)$$

The argument above, that  $d$  should be greater than unity in the presence of an erosion threshold, implies that  $\theta$  should be less than unity, as is usually observed (for a compilation of  $\theta$  values, see Tucker and Whipple, 2002). Values of concavity,  $\theta$ , from the study areas imply  $d$  in the vicinity of 3–6, which could be interpreted as indicating a strong degree of nonlinearity in the relationship between gradient and erosive potential. This is as expected given the substantial erosion threshold associated with grassland vegetation. Thus, the slope-area relationship in catchments in the study area (and likely other typical rangeland catchments) is consistent with our hypothesis that the observed network concavity reflects a balance between the frequency and magnitude of flash floods at different points within the network.

### Sensitivity to Climate Change

It is important to consider the sensitivity of arroyo networks to climate change. Given the importance of convective precipitation as a driving force and herbaceous vegetation as a

resisting factor, rates of valley incision should be particularly sensitive to convective activity and to drought-induced vegetation disturbance (Table 1). In the context of the American west, it is logical to expect that the greatest susceptibility to channel incision will occur when the return of convective summer rain marks the end of a significant drought cycle.

Holocene climate records from the southwestern United States are sometimes contradictory; for example, while the middle Holocene (ca. 5–7 ka) has historically been considered a warm and dry period in the southwestern United States (e.g., Waters, 1989; Davis and Schaefer, 1992; Waters and Haynes, 2001; Menking and Anderson, 2003), a variety of reconstructions point toward a maximum in summer monsoon rainfall during that period (Thompson et al., 1993; Metcalfe et al., 2000; Harrison et al., 2003; Poore et al., 2005). In any event, the predicted sensitivity of arroyo incision rates to both drought (via vegetation weakening) and summer thunderstorms is consistent with the observation of Waters and Haynes (2001) that arroyo activity in Arizona correlates with the strength of El Niño–Southern Oscillation (ENSO) cycles. It is also broadly consistent with dating of Holocene channel fills in the study areas (Arnold, 2006; Arnold et al., 2006), the results of which suggest more vigorous cut-fill behavior during the early-middle Holocene (as well as near the Pleistocene-Holocene boundary and the late Holocene neoglaciation).

Given the apparent importance of short-term climate variability, it is interesting to speculate on how longer-term variations in the degree of climate variability might impact denudation rates in rangeland settings. Significant denudation—on the order of several hundred meters (Leonard, 2002)—has occurred along the high plains east of the southern Rockies since the end of deposition of the Ogallala Group, ca. 5 Ma (e.g., Trimble, 1980). The mechanism for this denudation is the subject of much debate; some have attributed it to increased climate variability and/or storminess beginning in the Pliocene (Molnar and England, 1990; Gregory and Chase, 1994; Zhang et al., 2001). The apparent sensitivity of ephemeral channel incision rates to climate variability—specifically, alternating episodes of drought, which damages vegetation and can potentially reduce erosional resistance by an order of magnitude (Table 1), and intense summer convective storm activity, which generates high boundary shear stresses—provides a plausible mechanism for a climate-driven acceleration in denudation rates in the high plains. In order to properly evaluate this hypothesis, it will be necessary to quantify the relation between climatology and

long-term rates of hillslope and valley sediment transport and erosion in rangelands.

### ACKNOWLEDGMENTS

This research was supported by the U.S. Army Research Office (grants DAAD190110513, DAAD190110615, W911BF0410340), and by a cooperative agreement between Massachusetts Institute of Technology (MIT) and the Consiglio Nazionale delle Ricerche, Italy. This research would not have been possible without the generous logistical support of the Fort Carson Directorate of Environmental Compliance and Management; in particular, we thank Brian Goss, James Kulbeth, Jeff Linn, Bruce Miller, Linda Moeder, Caron Rififi, and Dan Sharps for assistance, enthusiasm, and insights. John Kuzmiak of the U.S. Geological Survey, Pueblo, kindly provided storm rainfall data. We are also grateful for field assistance from Mikael Attal, Nate Bradley, Domenico Capolongo, Quintijn Clevis, Daniel Collins, Nicole Gasparini, Salvatore Grimaldi, Vanessa Teles, and Vanessa Winchester. Finally, we thank Brian Goss, Alan Howard, and Ian Prosser for constructive and helpful review comments.

### REFERENCES CITED

- Antevs, E., 1952, Arroyo-cutting and filling: *The Journal of Geology*, v. 60, p. 375–385.
- Arkell, R.E., and Richards, F., 1986, Short duration rainfall relations for the western United States, in *Conference on Climate and Water Management*, North Carolina, American Meteorological Society, p. 136–141.
- Arnold, L.J., 2006, Optical dating and computer modelling of Arroyo epicycles in the American Southwest [Ph.D. thesis]: Oxford, School of Geography and the Environment, University of Oxford, 426 p.
- Arnold, L.J., Bailey, R.M., and Tucker, G.E., 2006, Statistical treatment of fluvial dose distributions from southern Colorado arroyo deposits: *Quaternary Geochronology*, (in press).
- Boardman, J., Parsons, A.J., Holmes, P.J., Holland, R., and Washington, R., 2003, Development of badlands and gullies in the Sneeuwberg, Great Karoo, South Africa: *Catena*, v. 50, no. 2–4, p. 165–184, doi: 10.1016/S0341-8162(02)00144-3.
- Buffington, J.M., and Montgomery, D.R., 1997, A systematic analysis of eight decades of incipient motion studies, with special reference to gravel-bedded rivers: *Water Resources Research*, v. 33, no. 8, p. 1993–2029, doi: 10.1029/97WR03190.
- Bull, L.J., Kirkby, M.J., Shannon, J., and Hooke, J.M., 2000, The impact of rainstorms on floods in ephemeral channels in southeast Spain: *Catena*, v. 38, p. 191–209, doi: 10.1016/S0341-8162(99)00071-5.
- Bull, W.B., 1997, Discontinuous ephemeral streams: *Geomorphology*, v. 19, p. 227–276, doi: 10.1016/S0169-555X(97)00016-0.
- Collins, D.B.G., Bras, R.L., and Tucker, G.E., 2004, Modeling the effects of vegetation-erosion coupling on landscape evolution: *Journal of Geophysical Research*, v. 109, F03004, doi: 10.1029/2003JF000028.
- Cooke, R.U., and Reeves, R.W., 1976, *Arroyos and environmental change in the American South-West*: London, Oxford University Press, 213 p.
- Crouch, R.J., and Novruzli, T., 1989, Threshold conditions for rill initiation on a vertisol, Gunnedah, N.S.W. Australia: *Catena*, v. 16, p. 101–110, doi: 10.1016/0341-8162(89)90007-6.
- Davis, O.K., and Schafer, D.S., 1992, A Holocene climatic record for the Sonoran Desert from pollen analysis of Montezuma Well, Arizona, USA: *Palaeogeography, Palaeoclimatology, Palaeoecology*, v. 92, p. 107–119.
- Dietrich, W.E., and Dunne, T., 1993, The channel head, in Beven, K., Kirkby, M.J., *Channel network hydrology*: Chichester, UK, John Wiley and Sons, p. 175–219.
- Dietrich, W.E., Wilson, C.J., Montgomery, D.R., and McKean, J., 1993, Analysis of erosion thresholds, channel networks, and landscape morphology using a digital

- terrain model: Centennial special issue: Chicago, Illinois, University of Chicago Press, p. 259–278.
- Elliott, J.G., Gellis, A.C., and Aby, S.B., 1999, Evolution of arroyos; incised channels of the Southwestern United States, *in* Darby, S.E., and Simon, A., eds., *Incised river channels*: Chichester, New York, John Wiley, p. 152–185.
- Elliott, W.J., Liebenow, A.M., Lafen, J.M., and Kohl, K.D., 1989, A compendium of soil erodibility data from WEPP cropland soil field erodibility experiments 1987 and 1988: W. Lafayette, Indiana, Ohio State University and USDA Agricultural Research Service National Soil Erosion Research Laboratory Report no. 3.
- Fanning, P.C., 1999, Recent landscape history in arid western New South Wales, Australia: a model for regional change: *Geomorphology*, v. 29, p. 191–209, doi: 10.1016/S0169-555X(99)00014-8.
- Farnsworth, K.L., and Milliman, J.D., 2003, Effects of climatic and anthropogenic change on small mountainous rivers: The Salinas River example: *Global and Planetary Change*, v. 39, p. 53–64, doi: 10.1016/S0921-8181(03)00017-1.
- Flores Cervantes, J.H., 2004, Headcut retreat resulting from plunge pool erosion in a 3D landscape evolution model [M.S. thesis]: Cambridge, Massachusetts Institute of Technology, 143 p.
- Foster, G.R., 1982, Modeling the erosion process, *in* Haan, C.T., ed., *Hydrologic modeling of small watersheds*: St. Joseph, Michigan, American Society of Agricultural Engineers Monograph 5, p. 295–380.
- Gilley, J.E., Elliott, W.F., Lafen, J.M., and Simanton, J.R., 1993, Critical shear stress and critical flow rates for initiation of rilling: *Journal of Hydrology*, v. 142, p. 251–271, doi: 10.1016/0022-1694(93)90013-Y.
- Goodrich, D.C., Lane, L.J., Shillito, R.M., and Miller, S.N., 1997, Linearity of basin response as a function of scale in a semiarid watershed: *Water Resources Research*, v. 33, no. 12, p. 2951–2965, doi: 10.1029/97WR01422.
- Graf, W.L., 1983, The arroyo problem: palaeohydrology and palaeohydraulics in the short term, *in* Gregory, K.L., ed., *Background to palaeohydrology: a perspective*: New York, John Wiley, p. 279–302.
- Graf, W.L., 1988, *Fluvial processes in dryland rivers*: Caldwell, New Jersey, Blackburn Press, 346 p.
- Gregory, K.M., and Chase, C.G., 1994, Tectonic and climatic significance of a late Eocene low-relief, high-level geomorphic surface: *Journal of Geophysical Research*, v. 99, p. B10, p. 20,141–20,160, doi: 10.1029/94JB00132.
- Hack, J.T., 1960, Interpretation of erosion topography in humid temperate climate: *American Journal of Science*, v. 258, p. 80–97.
- Harrison, S.P., Kutzbach, J.E., Liu, P., Bartlein, J.Z., Otto-Bliessner, B., Muhs, D., Prentice, I.C., and Thompson, R.S., 2003, Mid-Holocene climates of the Americas: a dynamical response to changed seasonality: *Climate Dynamics*, v. 20, p. 663–688.
- Howard, A.D., 1999, Simulation of gully erosion and bistable landforms, *in* Darby, S.E., and Simon, A., eds., *Incised river channels*: New York, John Wiley & Sons, p. 277–300.
- Howard, A.D., and Kerby, G., 1983, Channel changes in badlands: *Geological Society of America Bulletin*, v. 94, p. 739–752, doi: 10.1130/0016-7606(1983)94<739:CCIB>2.0.CO;2.
- Istanbulluoglu, E., Tarboton, D.G., Pack, R.T., and Luce, C.H., 2004, Modeling of the interactions between forest vegetation, disturbances and sediment yields: *Journal of Geophysical Research*, v. 109, F01009, doi: 10.1029/2003JF000041.
- Istanbulluoglu, E., Bras, R.L., Flores, H., and Tucker, G.E., 2005, Implications of bank failures and fluvial erosion for gully development: Field observations and modeling: *Journal of Geophysical Research*, v. 110, F01014, doi: 10.1029/2004JF000145.
- Kirkby, M.J., and Bull, L.J., 2000, Some factors controlling gully growth in fine-grained sediments: A model applied in southeast Spain: *Catena*, v. 40, p. 127–146, doi: 10.1016/S0341-8162(99)00077-6.
- Lague, D., Hovius, N., and Davy, P., 2005, Discharge, discharge variability, and the bedrock channel profile: *Journal of Geophysical Research*, v. 110, F04006, doi: 10.1029/2004JF000259.
- Leonard, E.M., 2002, Geomorphic and tectonic forcing of late Cenozoic warping of the Colorado piedmont: *Geology*, v. 30, no. 7, p. 595–598, doi: 10.1130/0091-7613(2002)030<0595:GATFOL>2.0.CO;2.
- Leopold, L.B., 1951, Rainfall frequency: An aspect of climatic variation: *Eos (Transactions, American Geophysical Union)*, v. 32, p. 347–357.
- Menking, K.M., and Anderson, R.Y., 2003, Contributions of La Niña and El Niño to middle Holocene drought and late Holocene moisture in the American Southwest: *Geology*, v. 31, p. 937–940.
- Merz, W., and Bryan, R.B., 1993, Critical conditions for rill initiation on sandy loam Brunisols: laboratory and field experiments in southern Ontario, Canada: *Geoderma*, v. 57(4), p. 357–385.
- Metcalfe, S.E., O'Hara, S.L., Caballero, M., and Davis, S.J., 2000, Records of late Pleistocene–Holocene climate change in Mexico—A review: *Quaternary Science Reviews*, v. 19, p. 699–721, doi: 10.1016/S0277-3791(99)00022-0.
- Miller, J.F., Frederick, R.H., and Tracey, R.J., 1973, *Precipitation-frequency atlas of the western United States*: Silver Spring, Maryland, National Oceanic and Atmospheric Administration, v. III, 67 p.
- Molnar, P., and England, P., 1990, Late Cenozoic uplift of mountain ranges and global climate change—Chicken or egg?: *Nature*, v. 346, no. 6279, p. 29–34, doi: 10.1038/346029a0.
- Molnar, P., Anderson, R.S., Kier, G., and Rose, J., 2006, Relationships among probability distributions of stream discharges in floods, climate, bedload transport and river incision: *Journal of Geophysical Research* (in press).
- Montgomery, D.R., and Dietrich, W.E., 1992, Channel initiation and the problem of landscape scale: *Science*, v. 255, no. 5046, p. 826–830.
- Moore, I.D., and Burch, G.J., 1986, Sediment transport capacity of sheet and rill flow: Application of unit stream power theory: *Water Resources Research*, v. 22, p. 1350–1360.
- Ogden, F.L., Sharif, H.O., Senarath, S.U.S., Smith, J.A., Baeck, M.L., and Richardson, J.R., 2000, Hydrologic analysis of the Fort Collins, Colorado, flash flood of 1997: *Journal of Hydrology*, v. 228, p. 82–100, doi: 10.1016/S0022-1694(00)00146-3.
- Oostwoud-Wijdenes, D., Poesen, J., Vandekerckhove, L., and De Baerdemaeker, J., 1999, Gully-head morphology and implications for gully development on abandoned fields in a semi-arid environment, Sierra de Gata, southeast Spain: *Earth Surface Processes and Landforms*, v. 24, p. 585–603, doi: 10.1002/(SICI)1096-9837(199907)24<585::AID-ESP976>3.0.CO;2-#.
- Patton, P.C., and Schumm, S.A., 1975, Gully erosion, northwestern Colorado: A threshold phenomenon: *Geology*, v. 3, p. 88–90, doi: 10.1130/0091-7613(1975)3<88:GENCAT>2.0.CO;2.
- Poore, R.Z., Pavich, M.J., and Grissino-Mayer, H.D., 2005, Record of the North American southwest monsoon from Gulf of Mexico sediment cores: *Geology*, v. 33, no. 3, p. 209–212, doi: 10.1130/G21040.1.
- Prosser, I.P., and Dietrich, W.E., 1995, Field experiments on erosion by overland flow and their implication for a digital terrain model of channel initiation: *Water Resources Research*, v. 31, no. 11, p. 2867–2876, doi: 10.1029/95WR02218.
- Prosser, I.P., and Slade, C.J., 1994, Gully formation and the role of valley-floor vegetation, southeastern Australia: *Geology*, v. 22, no. 12, p. 1127–1130, doi: 10.1130/0091-7613(1994)022<1127:GFATRO>2.3.CO;2.
- Prosser, I.P., Chappell, J., and Gillespie, R., 1994, Holocene valley aggradation and gully erosion in headwater catchments, south-eastern highlands of Australia: *Earth Surface Processes and Landforms*, v. 19, no. 5, p. 465–480.
- Prosser, I.P., Dietrich, W.E., and Stephenson, J., 1995, Flow resistance and sediment transport by concentrated overland flow in a grassland valley: *Geomorphology*, v. 13, p. 71–86, doi: 10.1016/0169-555X(95)00020-6.
- Ree, W.O., 1949, Hydraulic characteristics of vegetation for vegetated waterways: *Agricultural Engineering*, v. 30, p. 184–198.
- Reid, L.M., 1989, Channel initiation by surface runoff in grassland catchments: Seattle, University of Washington, 135 p.
- Reneau, S.L., Dietrich, W.E., Donahue, D.J., and Jull, A.J.T., 1990, Late Quaternary history of colluvial deposition and erosion in hollows, central California Coast Ranges: *Geological Society of America Bulletin*, v. 102, p. 969–982, doi: 10.1130/0016-7606(1990)102<0969:LQHOCD>2.3.CO;2.
- Rinaldo, A., Dietrich, W.E., Rigon, R., Vogel, G.K., and Rodriguez-Iturbe, I., 1995, Geomorphological signatures of varying climate: *Nature*, v. 374, no. 6523, p. 632–635, doi: 10.1038/374632a0.
- Schumm, S.A., 1977, *The fluvial system*: New York, John Wiley, 338 p.
- Schumm, S.A., Mosely, M.P., and Weaver, W.E., 1987, *Experimental fluvial geomorphology*: New York, John Wiley, 413 p.
- Schumm, S.A., and Parker, R.S., 1973, Implications of complex response of drainage systems for Quaternary alluvial stratigraphy: *Nature*, v. 243, no. 128, p. 99–100.
- Slattery, M.C., and Bryan, R.B., 1992, Hydraulic conditions for rill incision under simulated rainfall: *Earth Surface Processes and Landforms*, v. 17, p. 127–146.
- Slingerland, R.L., and Snow, R.S., 1988, Stability analysis of a rejuvenated fluvial system: *Zeitschrift für Geomorphologie*, v. 67, p. 93–102.
- Snow, R.S., and Slingerland, R.L., 1986, Mathematical modeling of graded river profiles: *Journal of Geology*, v. 95, p. 15–33.
- Snyder, N.P., Whipple, K.X., Tucker, G.E., and Merritts, D.J., 2003, The importance of a stochastic distribution of floods and erosion thresholds in the bedrock river incision problem: *Journal of Geophysical Research*, v. 108, no. B2, doi: 10.1029/2001JB001655.
- Stein, O.R., Julien, P.Y., and Alonso, C.V., 1993, Mechanics of jet scour downstream of a headcut: *Journal of Hydraulic Research*, v. 31, no. 6, p. 723–738.
- Thompson, R.S., Whitlock, C., Bartlein, P.J., Harrison, S.P., and Spaulding, W.G., 1993, Climate changes in the western United States since 18,000 yr B.P., *in* Wright, H. E., Jr., Kutzbach, J.E., Webb, T., III, Ruddiman, W.F., Street-Perrott, F.A., and Bartlein, P.J., eds., *Global climates since the Last Glacial Maximum*: Minneapolis, University of Minnesota Press, p. 468–513.
- Trimble, D.E., 1980, Cenozoic tectonic history of the Great Plains contrasted with that of the southern Rocky Mountains: A synthesis: *The Mountain Geologist*, v. 17, p. 59–69.
- Tucker, G.E., 2004, Drainage basin sensitivity to tectonic and climatic forcing: Implications of a stochastic model for the role of entrainment and erosion thresholds: *Earth Surface Processes and Landforms*, v. 29, p. 185–205, doi: 10.1002/esp.1020.
- Tucker, G.E., and Slingerland, R., 1997, Drainage basin responses to climate change: *Water Resources Research*, v. 33, no. 8, p. 2031–2047, doi: 10.1029/97WR00409.
- Tucker, G.E., and Whipple, K.X., 2002, Topographic outcomes predicted by stream erosion models: Sensitivity analysis and intermodel comparison: *Journal of Geophysical Research*, v. 107, no. B9, p. 2179, doi: 10.1029/2001JB000162.
- von Guerdard, P., Abbot, P.O., and Nickless, R.C., 1987, Hydrology of the US Army Pinon Canyon maneuver site, Las Animas County, Colorado: Denver, Colorado, Water-Resources Investigations Report 87-4227, U.S. Department of the Interior.
- Waters, M.R., 1989, Late Pleistocene and Holocene lacustrine history and paleoclimatic significance of pluvial Lake Cochise, southern Arizona: *Quaternary Research*, v. 32, p. 1–11.
- Waters, M.R., and Haynes, C.V., 2001, Late Quaternary arroyo formation and climate change in the American Southwest: *Geology*, v. 29, no. 5, p. 399–402, doi: 10.1130/0091-7613(2001)029<0399:LQAFAC>2.0.CO;2.
- Whipple, K.X., and Tucker, G.E., 1999, Dynamics of the stream-power river incision model; implications for height limits of mountain ranges, landscape response timescales, and research needs: *Journal of Geophysical Research*, ser. B, Solid Earth and Planets, v. 104, no. b8, p. 17,661–17,674, doi: 10.1029/1999JB900120.
- Willgoose, G., 1994, A Physical Explanation for an Observed Area-Slope-Elevation Relationship for Catchments with Declining Relief: *Water Resources Research*, v. 30(2), p. 15–159.
- Zhang, P., Molnar, P., and Downs, W.R., 2001, Increased sedimentation rates and grain sizes 2–4 Myr ago due to the influence of climate change on erosion rates: *Nature*, v. 410, no. 6831, p. 891–897, doi: 10.1038/35073504.

MANUSCRIPT RECEIVED 3 NOVEMBER 2005

REVISED MANUSCRIPT RECEIVED 3 FEBRUARY 2006

MANUSCRIPT ACCEPTED 20 FEBRUARY 2006

Printed in the USA